# Evaluation of the electrochemical anion recognition of NO3- -imprinted poly(Azure A) in NO3-/Cl- mixed solutions by ac-electrogravimetry

Jeronimo Agrisuelas, Claude Gabrielli, J.J. García-Jareño, Hubert Perrot, R. Sanchis-Gual, Ozlem Sel, F. Vicente

# Evaluation of the electrochemical anion recognition of $NO_3^-$-imprinted poly(Azure A) in $NO_3^-/Cl^-$ mixed solutions by *ac*-electrogravimetry

J. Agrisuelas*[,1], C. Gabrielli[2], J. J. García-Jareño[1], H. Perrot[2], R. Sanchis-Gual[1], O. Sel[2] and F. Vicente[1]

[1] Departament de Química Física, Universitat de València. C/ Dr. Moliner, 50, 46100, Burjassot, València, Spain.

[2] Sorbonne Universités, UPMC Univ Paris 06, CNRS, Laboratoire Interfaces et Systèmes Électrochimiques, 4 place Jussieu, F-75005, Paris, France.

*E-mail: jeronimo.agrisuelas@uv.es

**ABSTRACT**

During the reversible electrochemical reactions of the intrinsically conducting polymer (ICP) films, ions are inserted in them to balance the inner charge site of the polymer. For this reason, doped ICP films with anions or cations can be good candidates for the electrochemical removal of contaminant ions from wastewater. In this work, a polymer of a phenothiazine derivative (poly(Azure A or PAA)) was electrosynthesized by cyclic voltammetry in aqueous solutions using nitrate ions as a structural template. After that, PAA film was repeatedly cycled in identical conditions in a monomer-free solution. The electrochemical anion recognition of the nitrate-imprinted poly(Azure A) ($NO_3^-$-PAA) was evaluated by the combination of electrochemical and mass impedance spectroscopy, the so called *ac*-electrogravimetry method. *Ac*-electrogravimetry allows the selectivity of $NO_3^-$-PAA to be quantified. $NO_3^-$-PAA exhibited a special sensitivity and selectivity for the nitrate ions over the interfering chloride ions in mixed $NO_3^-$ and $Cl^-$ containing solutions. The Dixon plots of the kinetic constants obtained by *ac*-electrogravimetry were used as a graphical method to reveal that $NO_3^-$ and $Cl^-$ transfers are non-competitive at lower doped states of the polymer but competitive at higher doped states. The reversibility of nitrate incorporation controlled by an external potential modulation, the relative low cost and easy synthesis render the $NO_3^-$-PAA film suitable in practical implications such as nitrate scavenger in aqueous contaminated environments.

Keywords: Molecularly imprinted polymer; Electrochemical anion recognition; Electrochemical quartz crystal microbalance; poly(Azure A); Nitrate scavenger.

## 1. INTRODUCTION

Anions are involved in several important environmental and biological processes, as well as in the corrosion domain. However, anion accumulation in water can be very dangerous for human and animal health. Among all anions, nitrate in water is one of the most prevalent ecological problems since it is intensively used in pesticides and fertilizers [1–3]. Therefore, nitrate constitutes a large proportion of current pollutants in aqueous environments, specially, in regions with an intensive industrial activity [4,5]. In the last few years, urban groundwater has shown very similar or even higher nitrate concentrations than the areas traditionally dedicated to the agriculture [6]. Therefore, any new contribution concerning the nitrate removal from soils or water has a significant relevance.

In supramolecular chemistry, the interest in anion recognition have grown in recent years, with the development of new sensors or chemosensors [7–10]. The synthesis of molecularly imprinted polymers is an attractive method of creating recognition sites with memory to the target molecule in biological or aqueous media [11]. Molecularly imprinted polymers are synthetic macromolecular receptors that mimic the behavior of natural antibodies [12]. However, the technological design of these nanoscale devices requires large molecules with sophisticated molecular architectures and synthesis strategies [13].

Intrinsically conducting polymers (ICPs) are feasible alternatives for anion recognition in aqueous media owing to their environmental stability, low relative cost and good processability [14–17]. ICPs act as ion exchange membranes during the electrochemical reactions to maintain the inner electroneutrality [18]. Moreover, anion transfer can be externally controlled by a potential modulation. ICPs are easily synthetized with electrochemical methods by applying a fixed potential (potentiostatically), a fixed current (potentiometrically) or cycling the electrode potential (potentiodynamically). These methods are rather simple and allows the control of the film thickness with a uniform polymer distribution on the electrode surface [19]. This feature is particularly suitable for the coating of several kinds of electrodes from macroelectrodes to microelectrodes. Recently, Ramanavicius *et al.* proved that ICPs can be used for organic molecules recognition [20,21]. Specially, imprinted polypyrrole has been the most popular material in sensing application among the other ICPs for the inorganic anion

recognition [11]. This characteristic could be exploited to remove selectively nitrate from contaminated water using electrochemical techniques, and advantageously without generating additional species which normally occurs in the nitrate electrochemical reduction [22]. Moreover, the electrochemical reversibility of the anion insertion of ICPs is an important asset to reuse the imprinted polymer during repetitive decontamination processes.

Polyazines, macromolecules formed by the polymerization of dye molecules such as phenothiazines, phenoxazines or phenazines were increasingly used as redox mediators in sensors and biosensors [23]. However, the polyazines have not been intensively exploited as molecularly imprinted polymers. Contrary to the other ICPs with regular structures without cross-linked chains [24], polyazines provide highly complex and conjugated structure which are ideal structures for molecularly imprinted polymers with multitude of target analyte–polymer interactions (hydrogen bonding or electrostatic interaction) or specific cavities for the target analyte insertion [25]. Poly(Azure A) (PAA) is a phenothiazine derivative macromolecule resulting from the polymerization of the Azure A dye (Figure 1). After the polymerization, new bonds are generated to link the parent monomers because of a radical process. Recent works point out that this complex polymer has two different electroactive domains [26–29]. On one hand, the aromatic ring of AA preserves the pristine redox activity since the electroactivity of monomer is unaltered after the polymerization. On the other hand, new electroactive links involving N atoms from primary amino groups are formed between AA during the polymerization [23,30,31]. Each electroactive domain involves a two-electron transfer with a fast anion and a slow proton transfer in weak acid solutions [29]. Anions transfer involves a counter flux of free (not structural) water molecules caused by an exclusion effect. Both electroactive sites confer to PAA films a complex electrochemical mechanism, which was elucidated by hyphenated techniques in previous works where the anion plays an important role as counter-ion for charge balance during the electrochemical processes. The following equations show the proposed electrochemical mechanism of PAA films in weak acid aqueous solutions from the oxidized to the reduced PAA [29]:

$$[(\mathrm{PAA}^{\mathrm{ox}}_{\mathrm{link}})^{+}, \mathrm{A}^{-}] + \mathrm{e}^{-} \leftrightarrows \mathrm{PAA}^{*}_{\mathrm{link}} + \mathrm{A}^{-} \quad (1)$$

$$PAA^{*}_{link} + H^{+} + e^{-} \leftrightarrows PAA^{red}_{link} \quad (2)$$

$$\left[\left(PAA^{ox}_{ring}\right)^{+}, A^{-}\right] + e^{-} \leftrightarrows PAA^{*}_{ring} + A^{-} \quad (3)$$

$$PAA^{*}_{ring} + H^{+} + e^{-} \leftrightarrows PAA^{red}_{ring} \quad (4)$$

Herein, we report the electrosynthesis and characterization of nitrate-imprinted PAA films ($NO_3^-$-PAA) in two reference aqueous solutions containing either $NO_3^-$ or $Cl^-$, and three different mixed aqueous solution composed of both anions (competitive solutions with three different $NO_3^-/Cl^-$ ratios), which constitutes the first part of this work.

In the characterization or analytical studies of molecularly imprinted molecules, traditional electrochemical techniques are often employed; such as cyclic voltammetry or the electrochemical quartz crystal microbalance (EQCM) where global electrochemical responses are discussed [21,25]. Nowadays, both techniques exist more or less routinely in electrochemical laboratories. Distinguishing our study from these routine methods, the second part of this work consists of an evaluation of the kinetic and mechanistic aspects of anion transfer during the electrochemical activity of $NO_3^-$-PAA films by *ac*-electrogravimetry, a hyphenated electrochemical-mass impedance spectroscopy developed in a limited number of laboratories worldwide [32–35]. This coupling method dominates over the limitations of aforementioned traditional techniques and has the ability to deconvolute the global mass variations provided by classical EQCM measurements. To the best of our knowledge, this is the first time where $NO_3^-$-PAA is explored for its nitrate scavenging property by such an elaborated electrochemical method.

More specifically, *ac*-electrogravimetry consists of the in situ coupling of electrochemical impedance spectroscopy (EIS) and a fast EQCM. This technique simultaneously measures the mass/potential transfer function, $\Delta m/\Delta E(\omega)$ and the electrochemical impedance, $\Delta E/\Delta I(\omega)$ during a sinusoidal potential perturbation with a small amplitude applied to the modified working electrode. On the one hand, *ac*-electrogravimetry provides relevant information about the nature of species transferred at the solution|polymer interface discriminating between the charged and non-charged species and identifying anionic, cationic, and free solvent contributions during the

coupled electrochemical processes. On the other hand, one can obtain the kinetics of species transferred at the polymer|solution interface, and their transport in the bulk of the materials as well as their relative concentration within the polymer. Therefore, this hyphenated technique can extend the kinetics and mechanistic aspects of anion recognition on the electrochemistry of molecularly imprinted polymers. Although preliminary, the results presented here can be highly relevant to the preparation and exploitation of nitrate-imprinted PAA films in practical applications, especially in the context of selective removal of nitrate ions from wastewater.

## 2. EXPERIMENTAL

### 2.1. Materials

Azure A was purchased from Sigma. $KNO_3$ and KCl (analytical reagent) were purchased from Normapur. All standard solutions were freshly prepared with bi-distilled water.

### 2.2. Poly(Azure A) deposition

The polymer deposition was controlled by cyclic voltammetry in a typical three-electrodes cell. The reference electrode was a saturated calomel electrode (SCE, Tacussel XR 600) and all potentials are referred to it. The counter electrode was a platinum grid and the working electrode was a gold electrode with an electrode surface of 0.30 $cm^2$ patterned on a 9 MHz quartz crystal resonator (RAKON, France). The potentiostat/galvanostat was an Autolab PGSTAT302. The polymerization solution was a non deaereated 0.5 M $KNO_3$ and $5\times10^{-4}$ M AA (pH = 5). PAA was formed through 600 cycles between –0.6 V and +1.0 V with a 100 mV $s^{-1}$ scan rate. Then, the modified electrode was cycled under the same experimental conditions during 200 voltammetric cycles in a monomer-free 0.5 M $KNO_3$ solution which was purged with nitrogen during 5 min prior to the cycling, and kept under an inert atmosphere during the experiments.

### 2.3. *Ac*-electrogravimetry

*Ac*-electrogravimetry experiments were performed in two reference and three mixed aqueous solutions. The reference solutions consisted of 0.5 M $KNO_3$ ( $\chi_{NO_3^-} = 1$) and 0.5 M KCl ( $\chi_{NO_3^-} = 0$) aqueous solutions. The mixed solutions were prepared with

different $KNO_3$ fractions ( $\chi_{NO_3^-} = 0.7$, 0.5 and 0.3) where the ionic strength was kept constant at 0.5 M by addition of the appropriate amount of KCl, i.e. $\chi_{NO_3^-} = 0.7$ means a 0.35 M $KNO_3$ and 0.15 M KCl aqueous solution. The solutions were purged with nitrogen during 5 min before the cycling and were kept under inert nitrogen atmosphere during the acquisition of the *ac*-electrogravimetric spectra. For that, a four-channel Frequency Response Analyzer (FRA) Solartron 1254 and a SOTELEM-PGSTAT Z1 potentiostat were coupled with a fast EQCM. The $NO_3^-$-PAA modified working electrode was polarized at a given potential and a sinusoidal potential perturbation with a small amplitude (10 mV *rms*) was superimposed between 65 kHz and 0.01 Hz. The microbalance frequency change, $\Delta f_m$ and the alternating current response, $\Delta I$, were sent to the four channels FRA, which allowed the mass/potential transfer function, $\Delta m/\Delta E(\omega)$ and the electrochemical impedance, $\Delta E/\Delta I(\omega)$, to be simultaneously obtained. The experimental data were fitted to the theoretical expressions by means of Levenberg-Marquardt routines [36].

### 2.4. Vis-NIR cyclic spectroelectrochemistry

For the spectroelectrochemical characterization, the working electrode was a transparent indium-tin oxide (ITO) electrode with an active surface of 1 $cm^2$ (Glasstron, 30 $\Omega/cm^2$) where a $NO_3^-$-PAA film was synthetized under similar conditions. During certain voltammetric cycles, a vis-NIR spectrum was collected every 90 ms between 380 nm and 1080 nm by means of a StellarNet Inc SL1 equipment using a quartz cell with 10 mm light pass length as an electrochemical cell. In this occasion, solutions were not purged with inert nitrogen during the experiments.

## 3. RESULTS AND DISCUSSION

### 3.1. Electrogeneration of film

Cyclic voltammetry is the preferred electrochemical technique for monitoring the regular polymer growths [28]. In this work, PAA films have been electrosynthesized in 0.5 M $KNO_3$ aqueous solution through cyclic voltammetry. Figure 2a shows the typical current response during the electrosynthesis of this kind of polymer [37]. Between 0.8 V and 1.0 V, radical cations generated by the AA oxidation react among them resulting in the precipitation of polymer chains on the gold surface of the working electrode.

Undoubtedly, the molecular structure of Azure A has an important role in the growing polymer nanoarchitecture. Likewise, the trigonal planar structure of nitrate anions incorporated during the polymerization can also have a significant influence on the polymer nanostructure [38,39]. For a long time, it was established that the sort and size of counter-ions used in the polymerization strongly affect the physical and chemical properties of ICPs [40]. This fact is known as the template effect of the electrolyte anion since anions define the size and the shape of hydrated cavities inside the polymer [7].

The polymer electrodeposited on the gold electrode surface and the Azure A monomer in solution show their electrochemical activity in the potential range between 0.6 V and −0.6 V as shown in the current response evolution of the Figure 2a. During the PAA electrosynthesis, the current density corresponding to the deposited polymer increases every cycle up to the $450^{th}$ cycle. After that, the current density between 0.6 V and −0.6 V decreases to the value obtained at the last cycle. The electrochemical reactions of phenazine-like films become more difficult as the thickness increases due to a low electronic conductivity of this kind of polymers [41]. Despite this loss of electroactivity (Figure 2a), the increase in mass detected by EQCM is continuous during the electrosynthesis process (Figure 2b). It indicates that Azure A monomers are incorporated in the polymer chain, whereas the monomers are still available in the electrosynthesis solution. Finally, the mass deposited on the surface of the working electrode reaches 47 μg $cm^{-2}$. Using the commercial software ChemBio3D Ultra v. 12.0 Chem-BioOffice 2010, the volume of Azure A can be estimated from the Connolly Solvent Excluded Volume (168.335 $Å^3$). Thus, the estimated PAA thickness is about 185 nm. A thickness lower than c.a. 500 nm allows us keeping in the gravimetric range of EQCM [42].

### 3.2. $NO_3^-$ templating

To intensify the templating effect of nitrates, as-generated PAA film was repeatedly oxidized and reduced using cyclic voltammetry under identical conditions but in the Azure A-free 0.5 M $KNO_3$ aqueous solution. After 200 cycles, the PAA film shows a quasi-stable current response (Figure 3a). Like in Figure 2a, the electrosynthesized PAA shows an oxidation process at potentials higher than 0.8 V even without Azure A monomers in solution. Although this oxidation process continuously diminishes (i.e. current density decreases), it persists in the successive cycles. The radicalization of PAA chains can be a potential reason for this behavior. Therefore, an intrinsic oxidation process

of PAA can be considered feasible. Taking into account the monomer structure in Figure 1, the oxidation/radicalization of the primary and tertiary amino groups of the PAA chains is expected to result in the creation of new covalent bonds between polymeric segments [23,30,31]. Consequently, the cross-linking during the formation of $NO_3^-$ imprinted PAA film ($NO_3^-$-PAA) could be the cause of the reduction in the electrochemical response of about 35% with respect to the consumed charge in the first cycle (Figure 3a). During this partial inactivation, the mass increases up to the 100$^{th}$ cycle as shown in the Figure 3b. After that, the mass stabilizes between the 100$^{th}$ cycle to the 150$^{th}$ cycle and, then, decrease.

Considering Faraday's law, the instantaneous mass/charge ratio ($F(dm/dQ)$) evolution on the time scale allows us a better view of the nature of the instantaneous electrochemical processes to obtained. The molar mass of the species exchanged during the electrochemical processes is obtained through the transfer function $F(dm/dQ)$ [43]:

$$F\frac{dm/dt}{j} = F\frac{dm/dt}{dQ/dt} = F\frac{dm}{dQ} = -\sum \nu_i \frac{M_i}{z_i} \pm \xi \qquad (5)$$

where $F$ is the Faraday constant (96485 C mol$^{-1}$), $j$ is the current density, $m$ is the mass per area, $\nu_i$ represents the percentage (per unit) of the electrical charge balanced by the participation of the species $i$, $M_i$ is the molar mass of the species $i$ involved in the electrochemical processes, $Q$ is the charge associated to this process, $z_i$ is the number of electrons involved per active center in the electrochemical process and $\xi$ is the contribution due to the mass changes of the non-charged species involved in the electrochemical reactions. Considering a simplistic mechanism, $F(dm/dQ)$ is positive when the mass decreases during reduction and anions are involved in the reaction. On the contrary, $F(dm/dQ)$ is negative for cation transfer during the reduction process.

Figure 4 compares the evolution of $F(dm/dQ)$ in the first cycle and in the last cycle. In general, $F(dm/dQ)$ results are very similar to the results obtained elsewhere [29]. Here, the main differences observed in the $NO_3^-$-PAA film after repetitive voltammetric cycling in a monomer-free solution were discussed. The $F(dm/dQ)$ function around 0.9 V is +20 g mol$^{-1}$ in both cycles. it suggests the transfer of nitrate ions probably with a counter-flux of other species during the radicalization of PAA film. Assuming the loss of one electron during the radicalization of one electroactive site, the

insertion of one nitrate molecule involves the expulsion of about 2.3 free water molecules. Partial number of water molecules may be due to expansion/contraction of the PAA film during the electrochemical reactions [29,44]. However, we cannot discard the transfer of $OH^-$ with a theoretical $F(dm/dQ)$ of +17 g mol$^{-1}$.The cross-linking process during the radicalization at potentials higher than 0.8 V may hinder the expulsion of anions from sites buried deep inside the polymer in the next voltammetric cycle explaining the loss of the $NO_3^-$-PAA electroactivity and the mass gained during the first 100 cycles (Figure 3). Although the $NO_3^-$-PAA film is partially inactivated, a highly cross-linked PAA film can be obtained where the simultaneous $NO_3^-$ insertion for charge balance during the cross-linking process may reinforce the molecular architecture of the polymer. On the other hand, $F(dm/dQ)$ in the all potential range of the last cycle shows values about 10-20 g mol$^{-1}$ smaller than these ones in the all first cycle. It can be attributed to the expulsion of an extra molecule of free water during the anion insertion of the $NO_3^-$-PAA film and vice versa after 200 voltammetric cycles. Structural modifications of the film due to the cross-linking acquired by the repetitive voltammetric cycling may be the responsible of this additional free water transfer during the electrochemical reactions of the $NO_3^-$-PAA film.

The global spectroelectrochemical changes of a PAA film deposited on the transparent ITO electrode during the first voltammetric cycle of templating is shown in Figure 5a. The contour plot of the time-derivative absorbance ($dA/dt$)−polarization potential−wavelength between 410 and 1010 nm allows us selecting the wavelengths where PAA films show the most important electrochromic changes. $dA^\lambda/dt$ proves better for comparison with the electrical current by means of the Lambert−Beer law since both are proportional to the mol of electroactive sites such as:

$$j = \frac{dQ}{dt} = zF\frac{dn}{dt} \tag{6}$$

$$\frac{dA^\lambda}{dt} = \frac{d\left(\varepsilon^\lambda lc\right)}{dt} = \varepsilon^\lambda\frac{d\Gamma}{dt} = \frac{\varepsilon^\lambda}{S}\frac{dn}{dt} = \varepsilon'^\lambda\frac{dn}{dt} \tag{7}$$

where $n$ is mol of active sites, Γ is the apparente surface concnettration of electroactive sites, $l$ is the length of the light path, $S$ is the surface area of the electrode, $c$ is the volume concentration of active sites and $A^\lambda$ is the absorbance at a characteristics $\lambda$ wavelength.

The contour profile depicted in the Figure 5a during the first voltammetric cycle of templating remembers to previous results for PAA films, although electrosynthesized under different experimental conditions [26,28]. Therefore, a similar electrochemical mechanism as in eq (1)-(4) can be expected. The major electrochromic change takes place at 570 nm as shown in Figure 5a. However, the absorbance changes at 690 nm and 880 nm are the finest wavelengths to study the electrochromic behavior of PAA films: $A^{690\,nm}$ allows the color evolution between the uncolored form and colored forms of phenothiazine rings to be monitored whereas the $A^{880\,nm}$ allows the formation of the $PAA^{*}_{link}$ species during the reduction half-reaction in eq (1) ($[(PAA^{ox}_{link})^{+}, A^{-}] + e^{-} \rightarrow PAA^{*}_{link} + A^{-}$) and during the oxidation half-reaction in eq (2) ($PAA^{red}_{link} \rightarrow PAA^{*}_{link} + H^{+} + e^{-}$) to be identified.

Figure 5b shows a more detailed analysis of $dA^{\lambda}/dt$ curves at 570 nm, 690 nm and 880 nm before (straight line) and after (dashed line) the templating process of a PAA film in a monomer-free solution. In general, all $dA^{\lambda}/dt$ peaks after 200 cycles are smaller and wider than the ones in the first cycle. Moreover, the potential separation between $dA^{\lambda}/dt$ peaks increases after the repetitive cycling. The latter is due to the inactivation of the film, which increases the resistance of the modified electrode. A molecular change of the PAA film can be assumed, especially when the film is radicalized around 1 V. Moreover, it is important to note that $dA^{\lambda}/dt$ profiles of the first cycles in Figure 5b are slightly different that $dA^{\lambda}/dt$ of PAA films generated at slower potential scans [26–28]. Therefore, the polymer electrochemistry is also dictated by the synthesis conditions.

### 3.3. Electrochemical and mass transfer of nitrate-imprinted PAA films

During the induced electrochemical reactions of ICPs in aqueous solutions, doping/dedoping of anions balances the excess or defect of charges in the polymer films. The universally accepted concept of coupled electron/anion transfer is expressed as:

$$\langle P \rangle + A^{-} \underset{k'_{e^-}, k_{A^-}}{\overset{k_{e^-}, k'_{A^-}}{\rightleftharpoons}} \langle P^{+}, A^{-} \rangle + e^{-} \qquad (8)$$

where $\langle P \rangle$ is the dedoped polymer, $\langle P^{+}, A^{-} \rangle$ is the polymer doped with the anions $A^{-}$, and $k_{A^-}$ and $k_{e^-}$ are the kinetic constants of anion and electron expulsion from polymer,

respectively. Likewise, $k'_{A^-}$ and $k'_{e^-}$ are the kinetic constants of anion and electron insertion to polymer, respectively.

The kinetic constants only depend on the resistance of anions to cross the polymer|solution interface when the anions are transported fast enough through very thin films and in electrolytes with high ionic strength [45,46]. Then, the kinetic constants of both electron and anion transfer in the eq (8) are equal such as $k_{e^-} = k'_{A^-}$ and $k'_{e^-} = k_{A^-}$. Gabrielli *et al.* have extensively discussed these concepts when *ac*-electrogravimetry methods were used to investigate ionic transfer for very thin ICP films [45–50].

In this work, the competitive solutions consisted of different mole fractions of $NO_3^-$ and $Cl^-$. The $Cl^-$ species are intentionally chosen as an interfering ion for the following reasons:(i) $Cl^-$ is present in marine wastewater, (ii) the addition of $Cl^-$ allows the ionic strength of solution to be maintained constant avoiding significant concentration gradient, (iii) the small and spherical molecular geometry of $Cl^-$ do not electrochemically inactive the $NO_3^-$-PAA film since both ions can be inserted in the imprinted anion cavities of this film [29], and (iv) larger sized anions are avoided since they can lead to electrochemical inactivation of the molecularly imprinted polymer [7].

In a previous work from our group [29], it was proven that the major permselectivity domain of the $NO_3^-$-PAA film to anion transfer is induced in the potential range from 0.0 V to 0.6 V. Therefore, the *ac*-electrogravimetry responses of the $NO_3^-$ imprinted films were analyzed in a portion of this potential range between 0.05 V and 0.25 V. By subtracting the non-faradaic contributions, the experimental $\Delta q/\Delta E(\omega)$ response represented in a Cole-Cole diagram shows deformed semi-circles independent from the $NO_3^-$ concentration in solution (Figure 6a). As anion transfer in $NO_3^-$-PAA films is faster than proton transfer [29], the impedance spectra was only measured up to 160 mHz to focus on the frequency region where the charge transfer in the polymer is exclusively governed by the fast anion transfer. In this manner, we avoid the undesirable effect of proton transfer at lower frequencies. Moreover, the anion contribution during the electrochemical processes in this kind of polymers is maximized in weak acid solutions [51]. The experimental $\Delta m/\Delta E(\omega)$ response agrees with this assumption since it shows similar deformed semi-circles in the first quadrant as expected for the anion participation (Figure 6b) [52]. It is important to note that the electrochemical response in Figure 6a is very similar in all tested solutions. On the contrary, the $\Delta m/\Delta E(\omega)$ function

exhibits semi-circles where their diameters decrease as the $NO_3^-$ amount in the solution diminishes (Fig. 6b). A smaller diameter means that the mass change during the potential perturbation is smaller as it is expected in the reference solution containing only $Cl^-$, where $\gamma_{NO_3^-}/\gamma_{Cl^-} = 0$.

To evaluate the kinetics of anion transfers, an appropriate model which fits the experimental *ac*-electrogravimetry data was developed. In ref [29], we have extensively explained how to separate the kinetic aspects of the anion and excluded free water molecules in $Cl^-$ and $NO_3^-$ reference solutions. However, here in mixed solutions, a more complex theoretical model considering both anions transfer processes with their corresponding counter-flux of free water molecules is necessary which results in over-parameterized equations. Solving these equations involves several uncertainties and it is very challenging to evaluate the kinetics of the different species in these mixed solutions. From a practical point of view, the model was simplified considering an overall electrochemical process, thus to obtain an overall kinetic information under all experimental situations. This model was applied to all solutions by varying the $\gamma_{NO_3^-}/\gamma_{Cl^-}$ ratio

The transfer function $\Delta q/\Delta E(\omega)$ can be mathematically expressed as [50]:

$$\frac{\Delta q}{\Delta E}(\omega) = F\left[\frac{G}{(j\omega)^{\alpha} + K'}\right] \quad (9)$$

where $j = \sqrt{-1}$ and $\omega$ is the angular frequency which equals to $2\pi f$ where $f$ is the perturbation frequency. $K' = K/d_f$ is related to the kinetics constants in eq (8) of the electrochemical reaction where $K$ is the partial derivative of the flux of anions with respect to the potential, and $d_f$ represents the polymer film thickness. $G$ is the partial derivative of the flux of one species with respect to the concentration which can also be expressed as $G = (FR_{ct})^{-1}$ , and $R_{ct}$ represents the charge transfer resistance at the polymer|solution interface. Therefore, the $G$ parameter is related to the ease of species transfer through the polymer|solution interface during the electrochemical process.

Similarly, $\Delta m/\Delta E(\omega)$ is expressed as, using the same key parameters:

$$\frac{\Delta m}{\Delta E}(\omega) = -\frac{M_i}{z_i}\left[\frac{G}{(j\omega)^{\alpha} + K'}\right] \quad (10)$$

where $M$ is the averaged molar mass of the species involved during the overall electrochemical reaction. Characteristically, positive values are obtained if the mass decreases during the polymer reduction, which is due to the anion expulsion. These mathematical expressions have been extensively explained by Gabrielli *et al* [45,53].

Ideally, perfect semi-circles are obtained when $\alpha = 1$ in eq (10) or eq (11). It is important to highlight that the intention of this work is not to explain the meaning of the deviation from a perfect semicircle observed in $NO_3^-$-PAA. Thus, $(j\omega)^{\alpha}$ was considered as a mathematical resource to obtain the best fittings between the experimental results and the theoretical model. The solid lines in Figure 6 a and b show the best fitting achieved between the theoretical model and the raw data. Fortunately, homogenous values of $\alpha$ around 0.55±0.05 in all analyzed impedance spectra were obtained. This makes $K'$ and $G$ values among all experimental situations considered in this work comparable.

### 3.4. Selectivity of nitrate-imprinted PAA films

Figure 7 shows the evolution of $M$ defined in eq (8) in reference and mixed solutions in a potential range where anions are involved in the electrochemical reactions of polymer. As can be seen, $M$ decreases as the fraction of small anion ($Cl^-$) increases since more and more $Cl^-$ are inserted the electroactive sites. Likewise, $M$ decreases as $NO_3^-$-PAA is more and more reduced. That is due to the increasing participation of water transfer in the opposite direction of anion transfer as the polymer is less doped by anions [29]. On the other hand, $M$ in the $NO_3^-$ reference solution ($\chi_{NO_3^-} = 1$) and in the $Cl^-$ reference solution ($\chi_{NO_3^-} = 0$) does not correspond to the exact molar mass of $NO_3^-$ ($M_{NO_3^-}$ = 62 g mol$^{-1}$) or $Cl^-$ ($M_{Cl^-}$ = 35.5 g mol$^{-1}$). As demonstrated in a previous work [29], the simultaneous and opposite transfer of anion and free water molecules governed by the exclusion effect have to be considered. The expulsion of anions from the $NO_3^-$-PAA films leaves vacancies rapidly occupied by incoming free solvent molecules during the reduction reaction. On the contrary, anion insertion in the film involves the expulsion of a specific number of free water molecules from the hydrated cavities of the $NO_3^-$-PAA film. The exclusion effect is already and commonly proposed for other polymers, and the number of the excluded free solvent molecules depends on the size and the characteristics

of the anion transferred [54–57]. Moreover, the expansion/contraction of the polymer affects the transfer of the free water molecules and makes it difficult to estimate the film thickness [29,44,58]. In competitive solutions, the exclusion effect and the expansion/contraction of film also take place can be assumed.

Considering $M$ in both reference solutions as boundary conditions, the intermediate values of $M$ obtained in the mixed solutions are due to the participation of both anions which could competes by the electroactive sites and their corresponding counter flux of free water molecules. Considering both assumptions, the participation of each anion , $\gamma$, in the mixed solutions can be approximated following:

$$M^{E}_{\chi_{NO_3^-}} = \gamma_{NO_3^-}(M_1^E) + \gamma_{Cl^-}(M_0^E) \quad (11)$$

where $M^{E}_{\chi_{NO_3^-}}$ is $M$ at a certain potential $E$ in the $\chi_{NO_3^-}$ mixed solution characterized, $M_1^E$ is $M$ at a certain potential $E$ in the $NO_3^-$ reference solution ( $\chi_{NO_3^-} = 1$) and $M_0^E$ is $M$ at a certain potential $E$ in the $Cl^-$ reference solution ( $\chi_{NO_3^-} = 0$). $\gamma_{NO_3^-}$ is the partial contribution of nitrate to the global anion transfer, $\gamma_{Cl^-}$ is the partial contribution of chloride to the global anion transfer considering that $\gamma_{NO_3^-} + \gamma_{Cl^-} = 1$.

In unselective films, $\gamma_{NO_3^-}$ and $\gamma_{Cl^-}$ depend on the availability of anions in solution or, in other words, on the anion concentrations in the tested solutions. Therefore, it will be satisfied that $\chi_{Cl^-}/\gamma_{Cl^-} = \chi_{NO_3^-}/\gamma_{NO_3^-} = 1$ under such circumstances. On the contrary, if values far from the unity are found it means that films show a preference to insert one or the other anion from the mixed solutions. Therefore, these films can be selective for a certain anion. Now, the selectivity coefficient ($S$) can be defined as the ratio of partial contribution of anions divided by the ratio of anion concentrations in solution at every potential and is expressed by:

$$S = \frac{(\gamma_{NO_3^-}/\gamma_{Cl^-})}{(\chi_{NO_3^-}/\chi_{Cl^-})} \quad (12)$$

Therefore, $S$ is the unity in unselective films, if $S < 1$ then the film have a preference by $Cl^-$ but if $S > 1$ then the film prefers to insert $NO_3^-$.

Table 1 shows the calculated $S$ for the $NO_3^-$-PAA films at some polarization potentials in the three mixed solutions. In general, $NO_3^-$-PAA films prefer to insert nitrate anions since $S > 1$. In solutions with high nitrate ratio, values close to the unity at 0.05 V and 0.25 V are obtained. Therefore, the $NO_3^-$-PAA film is not excessively selective. However, $S$ value increases at intermediate polarization potentials in $\chi_{NO_3^-} = 0.7$ solution. At 0.15 and 0.2 V, the $NO_3^-$-PAA film preferentially inserts nitrate anions. In fact, it is expected that selectivity of the $NO_3^-$-PAA films will be evident at low concentration of nitrates in solution and therefore, for high $Cl^-$ concentration. This hypothesis is confirmed at 0.05 and 0.1 V and at lower $NO_3^-$ concentrations where $S$ reaches values close to 3. At these potentials, the $NO_3^-$-PAA film is partially doped with anions since the film is partially reduced, therefore, it has more vacancies to insert anions than in more oxidized states. Moreover, the polymer is partially protonated considering eq (2) which could facilitate the nitrate insertion. On the contrary, if the $NO_3^-$-PAA film is highly doped and deprotonated as at more anodic potentials, the preference of films to nitrates slightly decreases. However, these results show a general preference of the $NO_3^-$-PAA film for nitrate ions even at higher concentration of $Cl^-$. Therefore, we suggest that the anion binding recognition sites predominantly are cavities highly adapted to the trigonal planar structure of nitrate ions.

### 3.5. Blocking of nitrate binding sites in nitrate-imprinted PAA films

As an analogy, the incorporation of anions inside the $NO_3^-$ -PAA cavities can be related to the binding of an enzyme on a substrate. In a similar way, the nature of blocking of nitrate binding sites from the interfering $Cl^-$ ions can be evaluated using the Dixon plots [59]. Graphically, the lines converge on the same point on the X axis for a non-competitive blocking, on the contrary, the lines intersect above the X axis for a competitive blocking (Figure 8). Figure 9 shows the results when we plot the reciprocal values of the kinetics constants ($K'$ and $G$) obtained with eq (9)-(10) against the $Cl^-$ fraction (the blocker) in the mixed solution ($\chi_{Cl^-}$) at different potentials. In the present case, each potential corresponds to a specific concentration of free cavities, i.e. not occupied by anions, where anions can be inserted. The straight lines resulting of linear fittings (average $R^2 = 0.8 \pm 0.1$) allow us knowing the nature of blocking. The series of straight lines shown in Figure 9 agree with the reversible binding between the anions and the electroactive sites of the $NO_3^-$ -PAA films.

Taking as a reference the plots in Figure 8, the experimental Dixon plots in Figure 9 obtained from the results of *ac*-electrogravimetry have a mixed blocking. At potentials closer to 0 V, $Cl^-$ is a non-competitive blocker what means that $Cl^-$ inserted reduce the ability of $NO_3^-$ -PAA films to insert $NO_3^-$ probably changing the transfer rate of $NO_3^-$. At these potentials, the polymer is partially reduced, and, consequently, less doped with anions and partially protonated. Therefore, there are a great number of free cavities where anions can be inserted. As $NO_3^-$ -PAA film is more oxidized and, consequently, doped with anions and deprotonated, we observe an increasing competitive blocking since the lines intersect at intersect at $\chi_{Cl^-} = -0.1$ (Figure 9a) and $\chi_{Cl^-} = -0.25$ (Figure 9b). At these potentials (0.25 V and 0.2 V), anions compete for the small number of free cavities inside the film

### 3.6. Structural and optical properties of nitrate-imprinted PAA films

Spectroelectrochemistry can also help to understand the effect of anionic competitive solutions on the $NO_3^-$-PAA film electrochemistry. By combining the Lambert-Beer equation and Faraday's law, the molar absorptivity at $\lambda$ wavelength ($\varepsilon^{\lambda}$) of both electrochromic sites from $dA^{690}/dt$ and $dA^{880}/dt$ can be calculated [60,61]. In this work, the calculated extinction coefficient are used to discriminate some electrochemical processes during a voltammetric cycle such as the electrochemical process of eq (1) ($j_1(\mathrm{PAA}^{\mathrm{ox}}_{\mathrm{link}} \leftrightarrows \mathrm{PAA}^{*}_{\mathrm{link}})$), the electrochemical processes in eq (2)-(4) ($j_2\left(\mathrm{PAA}^{*}_{\mathrm{link}} \leftrightarrows \mathrm{PAA}^{\mathrm{red}}_{\mathrm{ring}}\right)$) and a parasitic reaction ($j_3$) such as the one demonstrated in ref [26]:

$$j_1 = z_1 F \frac{dn_{\mathrm{PAA}^{\mathrm{ox}}_{\mathrm{link}}}}{dt} = F\left(\frac{dA^{690}}{\varepsilon^{690} dt} - \frac{dA^{880}}{\varepsilon^{880} dt}\right) \tag{13}$$

$$j_2 = z_2 F \frac{dn_{\mathrm{PAA}^{\mathrm{red}}_{\mathrm{ring}}}}{dt} = 3F\left(\frac{dA^{690}}{\varepsilon^{690} dt}\right) \tag{14}$$

$$j_3 = j - (j_1 + j_2) \tag{15}$$

where $z_1$ =1 and $z_2$ =3 (the involved electrons in $j_1$ and $j_2$, respectively), $\varepsilon^{690}$ is $16\times10^6$ $cm^2\ mol^{-1}$, $\varepsilon^{880}$ is $9\times10^6$ $cm^2\ mol^{-1}$ and $j$ is the experimental current.

The simulated voltammograms (using eq (11)-(13)) for solutions with varying degree of $\chi_{NO_3^-}$ are shown in Figure 10. As it can be seen, the electrochemistry of the

$NO_3^-$-PAA films is very similar independent from the species and the anion fraction in the solution, at least with nitrate and chloride ions. Therefore, we can assume that the electrochemical mechanism in eq (1)-(4) is a general mechanism in weak acid solutions. Rigorously, the $NO_3^-$-PAA film shows slightly higher current density in nitrate solution ($\chi_{NO_3^-=1}$ in Figure 10a and Figure 10b) but this slight variation cannot be considered significant in both electrochemical processes. On the other hand, the parasitic reaction shown in Figure 10a is independent of the $NO_3^-$ or $Cl^-$ fraction in solution therefore anions are not involved [26]. These results underline the limitation of the cyclic voltammetry especially for the anion recognition of $NO_3^-$-PAA films. Thus, the *ac*-electrogravimetry results reported here are highly significant to establish a comprehensive understanding of ions transfer taking place during insertion/expulsion processes in mixed solutions.

## 4. CONCLUSIONS

In this work, a two-step synthesis strategy with the intention of obtaining $NO_3^-$-imprinted PAA or $NO_3^-$-PAA films is suggested. In a first step, pristine PAA films are electrochemically generated in 0.5 M $KNO_3$ solution with AA monomers. The molecular structure of Azure A and the trigonal planar structure of nitrate anions incorporated during the polymerization have a significant influence of the polymer nanoarchitecture. In a second step, PAA films are successively reduced and oxidized in a free-monomer 0.5 M $KNO_3$ solution to achieve a highly cross-linked polymer adapted to the $NO_3^-$ template. The electrochemical mechanisms of this film are very similar in $NO_3^-$ and $Cl^-$ reference solutions and in $NO_3^-/Cl^-$ mixed solutions, as shown by the spectroelectrochemistry results. Conversely, multi-scale coupled electrogravimetric methods (*ac*-electrogravimetry) enables to scrutinize the kinetic and mechanistic processes which take place during the electrochemical reactions of the $NO_3^-$-PAA films, especially in mixed $NO_3^-$ and $Cl^-$ solutions. Moreover, *ac*-electrogravimetry allows the selectivity of $NO_3^-$-PAA to be quantified. The analysis of kinetics values provided by *ac*-electrogravimetry using the Dixon plot prove clear that $NO_3^-$-PAA films have a higher affinity of this polymer towards $NO_3^-$ even in $NO_3^-/Cl^-$ mixed solutions. The $NO_3^-$ and $Cl^-$ ions transfers are non-competitive at lower doped states of the polymer. At higher doped states, both anions compete for the free cavities where they can be inserted during the charge balancing. Based on our findings, PAA can be included in the class of polymers forming molecularly imprinted polymer modified electrodes for applications in decontamination

processes. In the view of these promising results, the aim of future studies will be related to the optimization of the removal processes taking advantage of the $NO_3^-$-PAA films ability to selectively retain $NO_3^-$ in for example wastewater samples.


## ACKNOWLEDGMENTS

Part of this work was supported by CICyT project CTQ2011-28973/BQU.


## REFERENCES


[1] M.O. Rivett, S.R. Buss, P. Morgan, J.W.N. Smith, C.D. Bemment, Nitrate attenuation in groundwater: A review of biogeochemical controlling processes, Water Res. 42 (2008) 4215–4232.

[2] A. Costagliola, F. Roperto, D. Benedetto, A. Anastasio, R. Marrone, A. Perillo, V. Russo, S. Papparella, O. Paciello, Outbreak of fatal nitrate toxicosis associated with consumption of fennels (Foeniculum vulgare) in cattle farmed in Campania region (southern Italy), Environ. Sci. Pollut. Res. 21 (2014) 6252–6257.

[3] D.C. Gooddy, D.M.J. Macdonald, D.J. Lapworth, S.A. Bennett, K.J. Griffiths, Nitrogen sources, transport and processing in peri-urban floodplains, Sci. Total Environ. 494 (2014) 28–38.

[4] G.R. Hallberg, Agricultural chemicals in ground water: Extent and implications, American Journal of Alternative Agriculture. 2 (1987) 3–15.

[5] S.S.M. Hassan, H.E.M. Sayour, S.S. Al-Mehrezi, A novel planar miniaturized potentiometric sensor for flow injection analysis of nitrates in wastewaters, fertilizers and pharmaceuticals, Anal. Chim. Acta. 581 (2007) 13–18.

[6] F.T. Wakida, D.N. Lerner, Non-agricultural sources of groundwater nitrate: a review and case study, Water Res. 39 (2005) 3–16.

[7] K. Kamata, T. Suzuki, T. Kawai, T. Iyoda, Voltammetric anion recognition by a highly cross-linked polyviologen film, J. Electroanal. Chem. 473 (1999) 145–155.

[8] E.J. O'Neil, B.D. Smith, Anion recognition using dimetallic coordination complexes, Coordination Chemistry Reviews. 250 (2006) 3068–3080.

[9] A. Caballero, F. Zapata, P.D. Beer, Interlocked host molecules for anion recognition and sensing, Coordination Chemistry Reviews. 257 (2013) 2434–2455.

[10] N. Alizadeh, S. Nabavi, Synthesis and characterization of novel tetra cyclo[4]pyrrole ether as an anion recognition element for nanocomposite nitrate ion selective carbon paste electrode, Sens. Actuator B-Chem. 205 (2014) 127–135.

[11] X. Wu, Molecular imprinting for anion recognition in aqueous media, Microchim. Acta. 176 (2012) 23–47.

[12] C.S. Mahon, D.A. Fulton, Mimicking nature with synthetic macromolecules capable of recognition, Nat. Chem. 6 (2014) 665–672.

[13] S. Kubik, C. Reyheller, S. Stüwe, Recognition of Anions by Synthetic Receptors in Aqueous Solution, J. Incl. Phenom. Macrocycl. Chem. 52 (2005) 137–187.

[14] G. Inzelt, Mechanism of Charge Transport in Polymer Modified Electrodes, in: Bard, A. J. (Ed.), Electroanalytical Chemistry, A Series of Advances, Marcel Dekker, Inc., New York, 1993: pp. 89–241.

[15] M.E.G. Lyons, Electroactive Polymer Electrochemistry, Part 1: Fundamentals, 1st ed., Springer, New York, 1995.

[16] M.E.G. Lyons, Electroactive Polymer Electrochemistry: Part 2: Methods and Applications, Springer, 1996.
[17] G. Inzelt, M. Pineri, J.W. Schultze, M.A. Vorotyntsev, Electron and proton conducting polymers: recent developments and prospects, Electrochim. Acta. 45 (2000) 2403–2421.
[18] T.V. Shishkanova, I. Sapurina, J. Stejskal, V. Kral, R. Volf, Ion-selective electrodes: Polyaniline modification and anion recognition, Anal. Chim. Acta. 553 (2005) 160–168.
[19] J. Rishpon, S. Gottesfeld, Investigation of Polypyrrole Glucose-Oxidase Electrodes by Ellipsometric, Microgravimetric and Electrochemical Measurements, Biosens. Bioelectron. 6 (1991) 143–149.
[20] I. Baleviciute, V. Ratautaite, A. Ramanaviciene, Z. Balevicius, J. Broeders, D. Croux, M. McDonald, F. Vahidpour, R. Thoelen, W.D. Ceuninck, K. Haenen, M. Nesladek, A. Reza, A. Ramanavicius, Evaluation of theophylline imprinted polypyrrole film, Synth. Met. 209 (2015) 206–211.
[21] V. Ratautaite, D. Plausinaitis, I. Baleviciute, L. Mikoliunaite, A. Ramanaviciene, A. Ramanavicius, Characterization of caffeine-imprinted polypyrrole by a quartz crystal microbalance and electrochemical impedance spectroscopy, Sensors and Actuators B: Chemical. 212 (2015) 63–71.
[22] F. Vicente, J.J. García-Jareño, R. Tamarit, A. Cervilla, A. Domenech, Electrochemical Reduction of the Nitrite to Ammonium-Ions in Presence of $[MoO_2(O_2CC(S)C_6H_5)_2]^{2-}$, Electrochim. Acta. 40 (1995) 1121–1126.
[23] R. Pauliukaite, M.E. Ghica, M.M. Barsan, C.M.A. Brett, Phenazines and Polyphenazines in Electrochemical Sensors and Biosensors, Anal. Lett. 43 (2010) 1588–1608.
[24] Y. Wang, Research progress on a novel conductive polymer–poly(3,4-ethylenedioxythiophene) (PEDOT), J. Phys.: Conf. Ser. 152 (2009) 012023.
[25] Y.V. Ulyanova, A.E. Blackwell, S.D. Minteer, Poly(methylene green) employed as molecularly imprinted polymer matrix for electrochemical sensing, Analyst. 131 (2006) 257–261.
[26] J. Agrisuelas, D. Giménez-Romero, J.J. García-Jareño, F. Vicente, Vis/NIR spectroelectrochemical analysis of poly-(Azure A) on ITO electrode, Electrochem. Commun. 8 (2006) 549–553.
[27] J. Agrisuelas, C. Gabrielli, J.J. Garcia-Jareño, D. Gimenez-Romero, H. Perrot, F. Vicente, Spectroelectrochemical identification of the active sites for protons and anions insertions into poly-(Azure a) thin polymer films, J. Phys. Chem. C. 111 (2007) 14230–14237.
[28] J. Agrisuelas, J.J. García-Jareño, D. Gimenez-Romero, F. Vicente, An approach to the electrochemical activity of poly-(phenothiazines) by complementary electrochemical impedance spectroscopy and Vis–NIR spectroscopy, Electrochim. Acta. 55 (2010) 6128–6135.
[29] J. Agrisuelas, C. Gabrielli, J.J. Garcia-Jareño, H. Perrot, F. Vicente, Ionic and Free Solvent Motion in Poly(azure A) Studied by ac-Electrogravimetry, J. Phys. Chem. C. 115 (2011) 11132–11139.
[30] M.M. Barsan, E.M. Pinto, C.M.A. Brett, Electrosynthesis and electrochemical characterisation of phenazine polymers for application in biosensors, Electrochim. Acta. 53 (2008) 3973–3982.
[31] M.M. Barsan, E.M. Pinto, C.M.A. Brett, Methylene blue and neutral red electropolymerisation on AuQCM and on modified AuQCM electrodes: an

electrochemical and gravimetric study, Phys. Chem. Chem. Phys. 13 (2011) 5462–5471.
[32] A. Rubin, H. Perrot, C. Gabrielli, M.C. Pham, B. Piro, Electrochemical and electrogravimetric behaviors of conducting polymer. Theoretical aspects and application to co-polymer films based on juglone, Electrochim. Acta. 55 (2010) 6136–6146.
[33] L.T.T. Kim, O. Sel, C. Debiemme-Chouvy, C. Gabrielli, C. Laberty-Robert, H. Perrot, C. Sanchez, Proton transport properties in hybrid membranes investigated by ac-electrogravimetry, Electrochem. Commun. 12 (2010) 1136–1139.
[34] C. Benmouhoub, J. Agrisuelas, N. Benbrahim, F. Pillier, C. Gabrielli, A. Kadri, A. Pailleret, H. Perrot, O. Sel, Influence of the Incorporation of CeO2 Nanoparticles on the Ion Exchange Behavior of Dodecylsulfate Doped Polypyrrole Films: Ac-Electrogravimetry Investigations, Electrochim. Acta. 145 (2014) 270–280.
[35] F. Razzaghi, C. Debiemme-Chouvy, F. Pillier, H. Perrot, O. Sel, Ion intercalation dynamics of electrosynthesized mesoporous WO3 thin films studied by multi-scale coupled electrogravimetric methods, Phys. Chem. Chem. Phys. 17 (2015) 14773–14787.
[36] J.R. Macdonald, Comparison and application of two methods for the least squares analysis of immittance data, Solid State Ion. 58 (1992) 97–107.
[37] A.A. Karyakin, E.E. Karyakina, H.-L. Schmidt, Electropolymerized Azines: A New Group of Electroactive Polymers, Electroanal. 11 (1999) 149–155.
[38] A. Elmansouri, A. Outzourhit, A. Lachkar, N. Hadik, A. Abouelaoualim, M.E. Achour, A. Oueriagli, E.L. Ameziane, Influence of the counter ion on the properties of poly(o-toluidine) thin films and their Schottky diodes, Synth. Met. 159 (2009) 292–297.
[39] E. Poverenov, M. Li, A. Bitler, M. Bendikov, Major Effect of Electropolymerization Solvent on Morphology and Electrochromic Properties of PEDOT Films, Chem. Mater. 22 (2010) 4019–4025.
[40] K. Naoi, M. Lien, W.H. Smyrl, Quartz Crystal Microbalance Study: Ionic Motion Across Conducting Polymers, J. Electrochem. Soc. 138 (1991) 440–445.
[41] R. Pauliukaite, C.M.A. Brett, Poly(neutral red): Electrosynthesis, characterization, and application as a redox mediator, Electroanal. 20 (2008) 1275–1285.
[42] S. Bruckenstein, J. Chen, I. Jureviciute, A.R. Hillman, Ion and solvent transfers accompanying redox switching of polypyrrole films immersed in divalent anion solutions, Electrochim. Acta. 54 (2009) 3516–3525.
[43] D. Giménez-Romero, J.J. García-Jareño, F. Vicente, EQCM and EIS studies of $Zn_{aq}^{2+}+2e^{-}\rightleftarrows Zn^{0}$ electrochemical reaction in moderated acid medium, J. Electroanal. Chem. 558 (2003) 25–33.
[44] J. Agrisuelas, C. Gabrielli, J.J. García-Jareño, H. Perrot, O. Sel, F. Vicente, Polymer dynamics in thin p-type conducting films investigated by ac-electrogravimetry. Kinetics aspects on anion exclusion, free solvent transfer, and conformational changes in poly(o-toluidine), Electrochim. Acta. 153 (2015) 33–43.
[45] C. Gabrielli, J.J. García-Jareño, M. Keddam, H. Perrot, F. Vicente, Ac-Electrogravimetry Study of Electroactive Thin Films. I. Application to Prussian Blue, J. Phys. Chem. B. 106 (2002) 3182–3191.
[46] C. Gabrielli, J.J. Garcia-Jareño, M. Keddam, H. Perrot, F. Vicente, Ac-Electrogravimetry Study of Electroactive Thin Films. II. Application to Polypyrrole, J. Phys. Chem. B. 106 (2002) 3192–3201.
[47] C. Gabrielli, M. Keddam, N. Nadi, H. Perrot, ac Electrogravimetry on conducting polymers. Application to polyaniline, Electrochim. Acta. 44 (1999) 2095–2103.

[48] C. Gabrielli, M. Keddam, N. Nadi, H. Perrot, Ions and solvent transport across conducting polymers investigated by ac electrogravimetry. Application to polyaniline, J. Electroanal. Chem. 485 (2000) 101–113.
[49] C. Gabrielli, J. Garcia-Jareño, H. Perrot, Charge transport in electroactive thin films investigated by ac electrogravimetry, ACH-Models Chem. 137 (2000) 269–297.
[50] C. Gabrielli, H. Perrot, A. Rubin, M.C. Pham, B. Piro, Ac-electrogravimetry study of ionic exchanges on a polypyrrole modified electrode in various electrolytes, Electrochem. Commun. 9 (2007) 2196–2201.
[51] D. Benito, C. Gabrielli, J.J. García-Jareño, M. Keddam, H. Perrot, F. Vicente, An electrochemical impedance and ac-electrogravimetry study of PNR films in aqueous salt media, Electrochem. Commun. 4 (2002) 613–619.
[52] J. Agrisuelas, J.J. Garcia-Jareño, D. Gimenez-Romero, F. Vicente, Innovative Combination of Three Alternating Current Relaxation Techniques: Electrical Charge, Mass, and Color Impedance Spectroscopy. Part I: The Tool, J. Phys. Chem. C. 113 (2009) 8430–8437.
[53] C. Gabrielli, H. Perrot, Modeling and Numerical Simulations II, in: Schlesinger, M. (Ed.), In Modern Aspects of Electrochemistry, Springer, New York, 2009: p. 151−238.
[54] A. Hillman, D. Loveday, M. Swann, S. Bruckenstein, C. Wilde, Transport of Neutral Species in Electroactive Polymer-Films, J. Chem. Soc., Faraday Trans. 87 (1991) 2047–2053.
[55] A. Hillman, D. Loveday, M. Swann, S. Bruckenstein, C. Wilde, Mobile Species Uptake by Polymer-Modified Electrodes, Analyst. 117 (1992) 1251–1257.
[56] W. Plieth, A. Bund, U. Rammelt, S. Neudeck, L.M. Duc, The role of ion and solvent transport during the redox process of conducting polymers, Electrochim. Acta. 51 (2006) 2366–2372.
[57] J. Agrisuelas, C. Gabrielli, J.J. García-Jareño, H. Perrot, F. Vicente, Effects of anion size on the electrochemical behavior of H2SO4-structured poly(o-toluidine) films. An ac-electrogravimetry study in acid solutions, Electrochim. Acta. 132 (2014) 561–573.
[58] J. Agrisuelas, C. Gabrielli, J.J. García-Jareño, H. Perrot, O. Sel, F. Vicente, Electrochemically induced free solvent transfer in thin poly(3,4-ethylenedioxythiophene) films, Electrochim. Acta. 164 (2015) 21–30.
[59] M. Dixon, The Determination of Enzyme Inhibitor Constants, Biochem. J. 55 (1953) 170–171.
[60] S.I.C. de Torresi, The effect of manganese addition on nickel hydroxide electrodes with emphasis on its electrochromic properties, Electrochim. Acta. 40 (1995) 1101–1107.
[61] W.A. Gazotti Jr., M.J.D.M. Jannini, S.I. Córdoba de Torresi, M.-A. De Paoli, Influence of dopant, pH and potential on the spectral changes of poly(o-methoxyaniline): relationship with the redox processes, J. Electroanal. Chem. 440 (1997) 193–199.

**TABLES**

Table 1. Selectivity coefficient ($S$) calculated with eq (12) for a $NO_3^-$-PAA film at different polarization potentials in three $NO_3^-/Cl^-$ competitive solutions.

| $\chi_{NO_3^-}$ | $\chi_{Cl^-}$ | $S$ | | | | |
|---|---|---|---|---|---|---|
| | | 0.05 V | 0.1 V | 0.15 V | 0.2 V | 0.25V |
| 0.7 | 0.3 | 1.1 | 1.3 | 1.6 | 1.8 | 1.3 |
| 0.5 | 0.5 | 2.6 | 2.6 | 2.2 | 2.0 | 1.6 |
| 0.3 | 0.7 | 2.6 | 2.4 | 2.1 | 2.3 | 2.0 |

**FIGURES CAPTIONS**

Figure 1. Chemical structure of the Azure A monomer.

Figure 2. Repetitive cyclic voltammetry (a) for the electrosynthesis of PAA films on gold electrodes in 0.5 M $KNO_3$ aqueous solution containing $5\times10^{-4}$ M AA where it is shown every 40 cycles. Mass changes (b) during the electrosynthesis of PAA films where it is shown every 10 cycles. The scan rate was 100 mV $s^{-1}$ at room temperature and pH=5.

Figure 3. Repetitive cyclic voltammetry (a) of a PAA films deposited on gold electrodes in 0.5 M $KNO_3$ aqueous solution where it is shown every 40 cycles. Mass changes (b) during the cyclic voltammetry of PAA films where it is shown every 10 cycles. The scan rate was 100 mV $s^{-1}$ at room temperature without oxygen and pH = 5.

Figure 4. $F(dm/dQ)$ function *vs* potential of a PAA-gold modified electrode in $KNO_3$ 0.5 M at room temperature and pH=5 of the first and last voltammetric cycle of Figure 3. Open symbols draw the oxidation direction and filled symbols are the reduction direction.

Figure 5. 3D contour plot of time-derivative absorbance ($dA/dt$)−polarization potential−wavelength between 410 and 1010 nm during the first voltammetric cycle of a PAA-ITO modified electrode in $KNO_3$ 0.5 M at room temperature and pH=5 (a) and $dA^{\lambda}/dt$ curves at 570 nm, 690 nm and 880 nm during the first (straight line) and 200$^{th}$ (dashed line) voltammetric cycle (b) for a PAA-ITO modified electrode in $KNO_3$ 0.5 M at room temperature and pH=5. One vis-NIR spectrum was collected every 90 ms. Dashed lines in (b) are original values multiplied by 4 to have visual comparable values.

Figure 6. $\Delta q/\Delta E\ (\omega)$ (a) and $\Delta m/\Delta E\ (\omega)$ (b) of a $NO_3^-$-PAA film at E= +0.1 V in $NO_3^-$ and $Cl^-$ reference solutions and in one $NO_3^-/Cl^-$ mixed solution at room temperature and pH=5. The continuous lines are the theoretical curves from fittings using eq (9) and (10).

Figure 7. Evolution of averaged molar mass of the species involved during the overall electrochemical reaction, $M$, calculated from eq (10) at different potentials in $NO_3^-$ and $Cl^-$ reference solutions and in three $NO_3^-/Cl^-$ mixed solutions.

Figure 8. Theoretical Dixon plots for a non-competitive blocking (left) and for a competitive blocking (right).

Figure 9. Dixon plots of the $K'$ parameter (a) and the $G$ parameter (b) obtained by fitting experimental impedances from Figure 6 spectra with the theoretical model using eq (9) and (10) for a $NO_3^-$-PAA film in $NO_3^-$ and $Cl^-$ reference solutions and in three $NO_3^-/Cl^-$ mixed solutions. The continuous lines are linear fittings to guides to the eye.

Figure 10. Simulated voltammograms of the $PAA_{link}^{ox} \leftrightarrows PAA_{link}^{*}$ process ($j_1$ in a), $PAA_{link}^{*} \leftrightarrows PAA_{ring}^{red}$ process ($j_2$ in b) and parasitic reaction ($j_3$ in c) for a $NO_3^-$-PAA film in $NO_3^-$ and $Cl^-$ reference solutions and in three $NO_3^-/Cl^-$ competitive solutions at room temperature and pH=5.

**FIGURES**

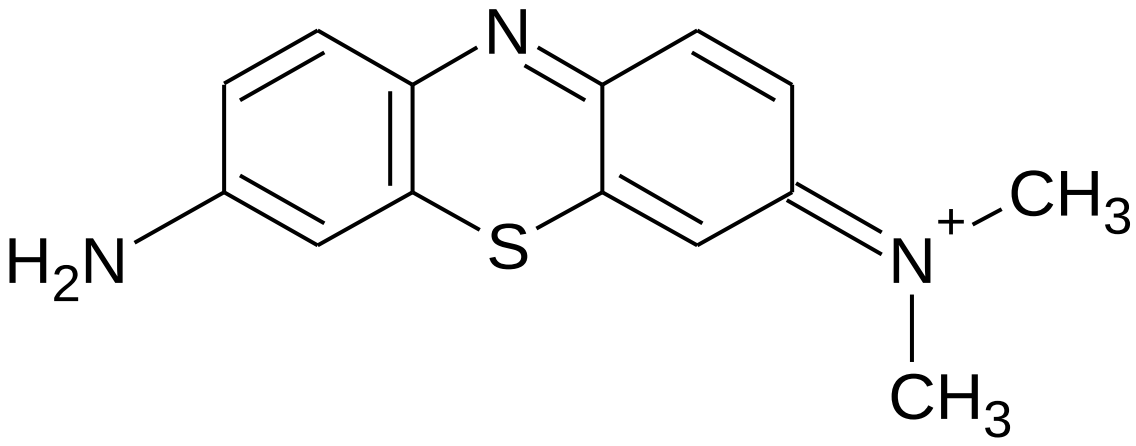


Figure 1

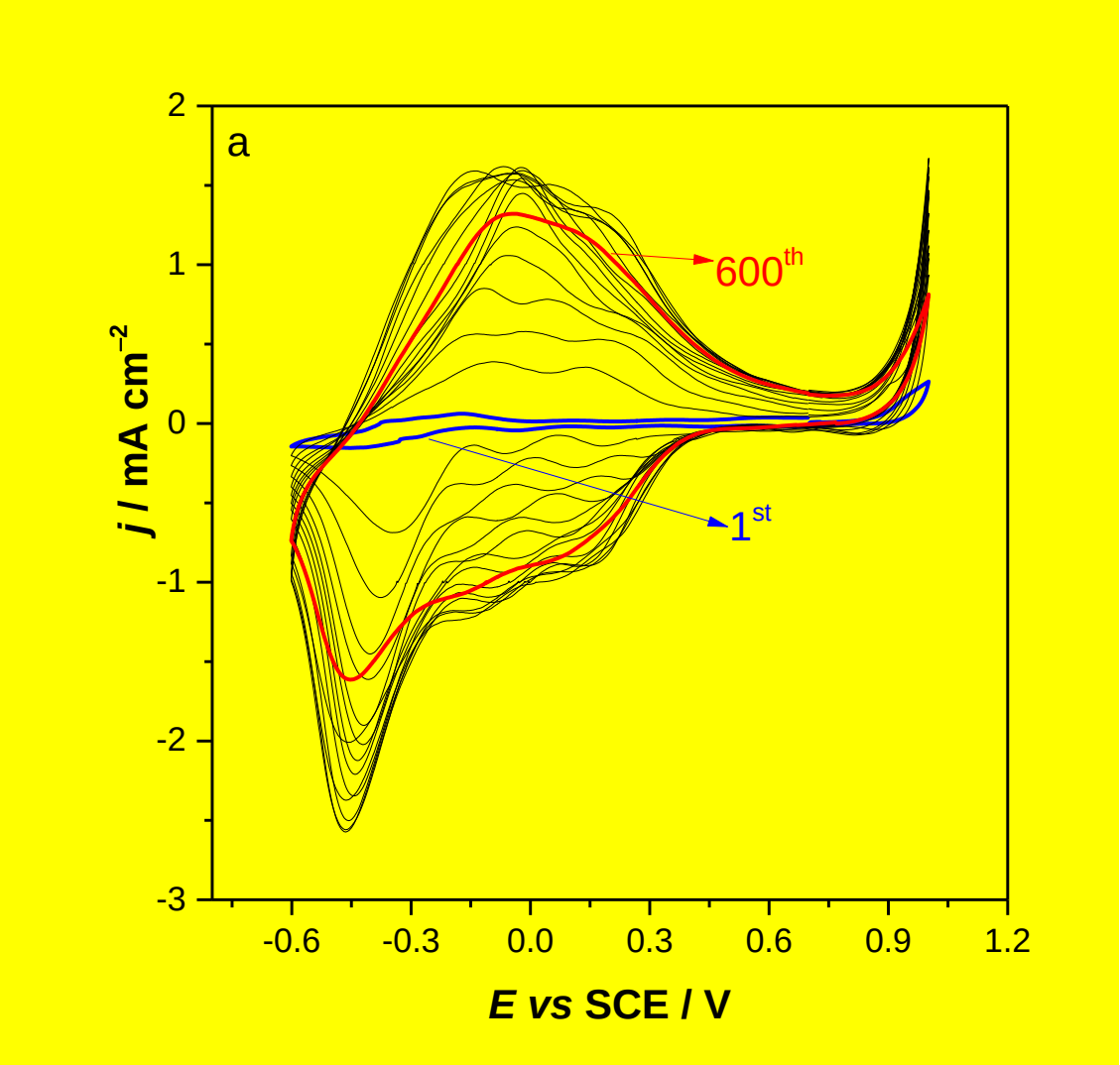


Figure 2a

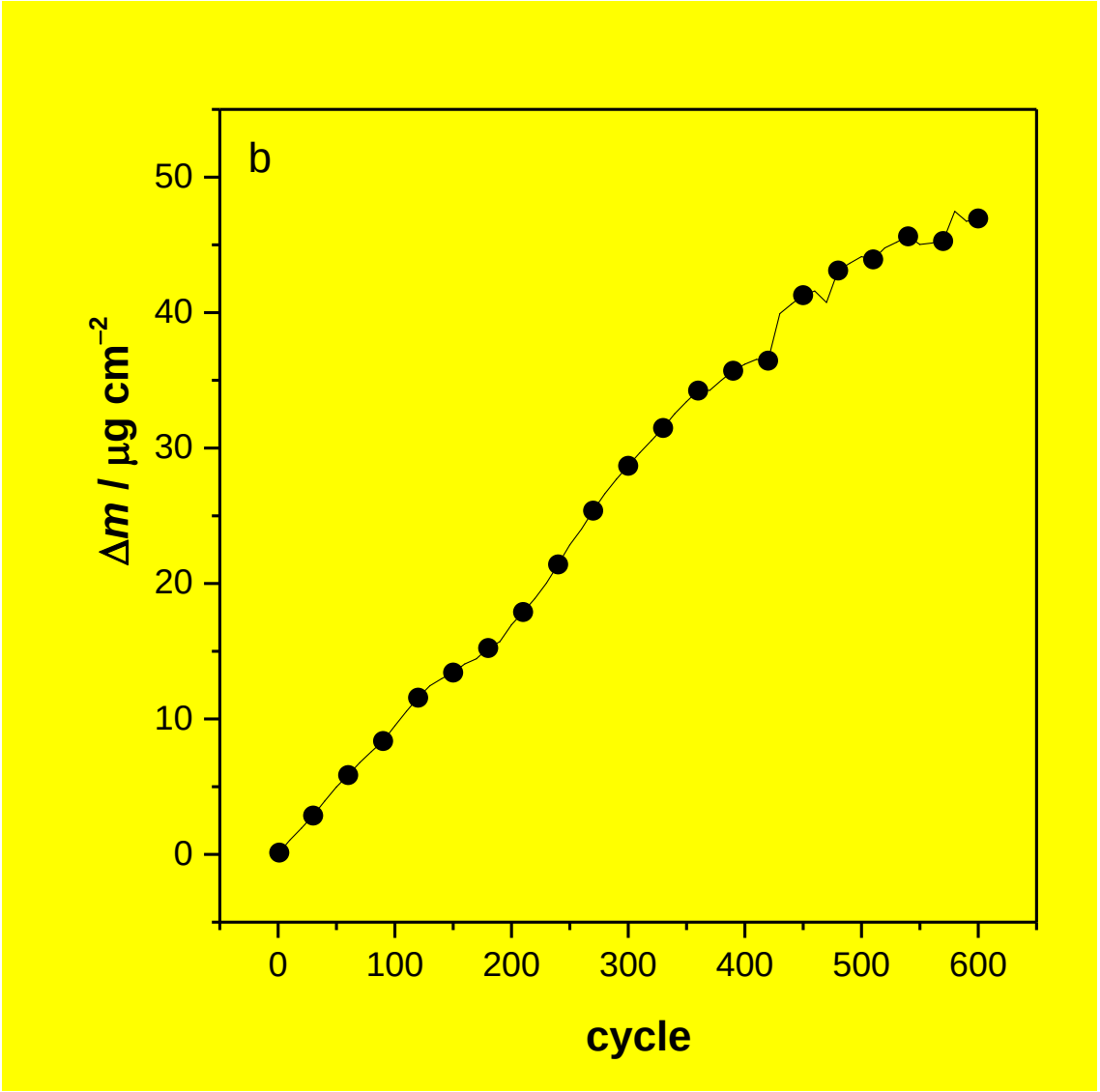


Figure 2b

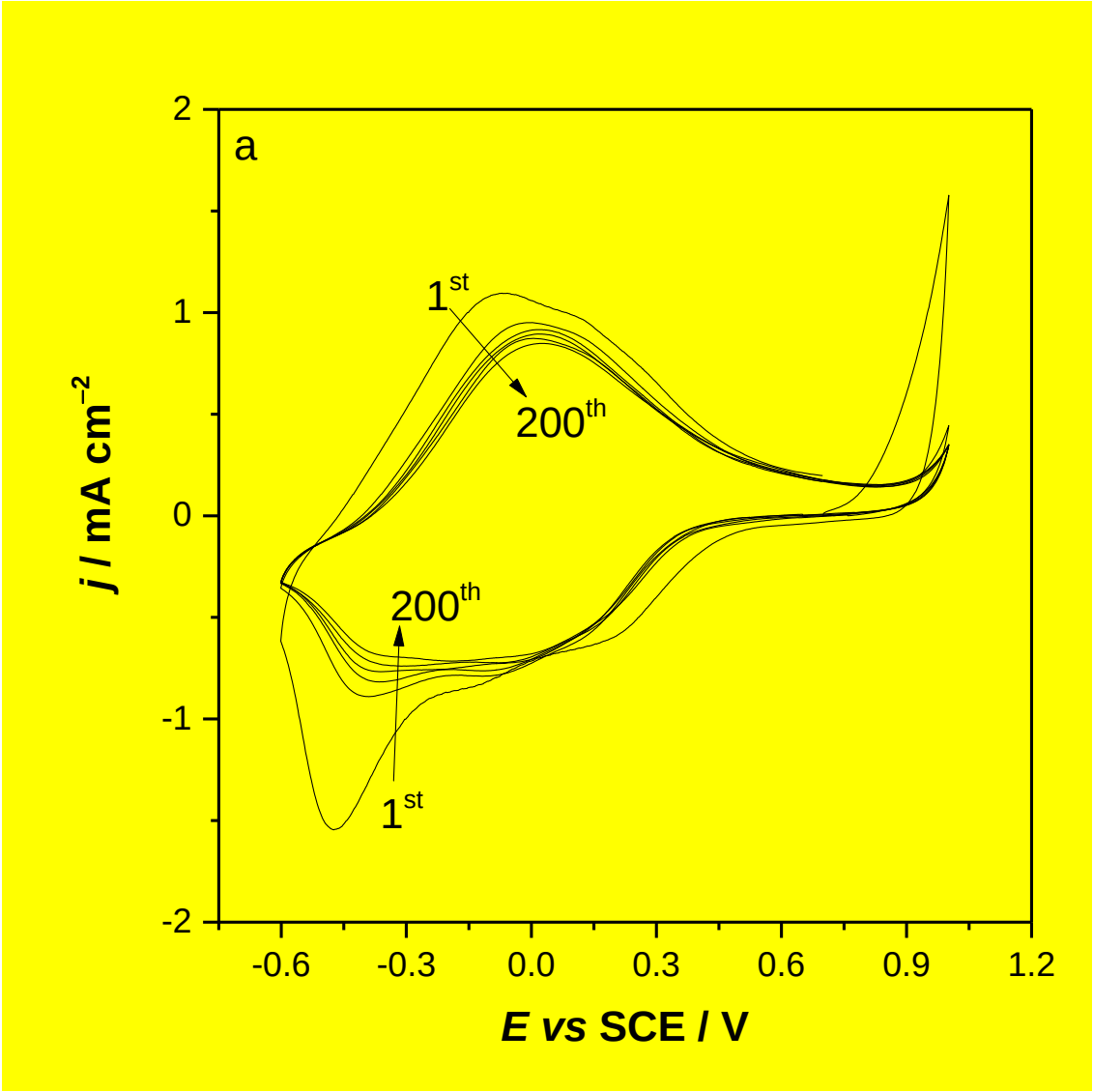


Figure 3a

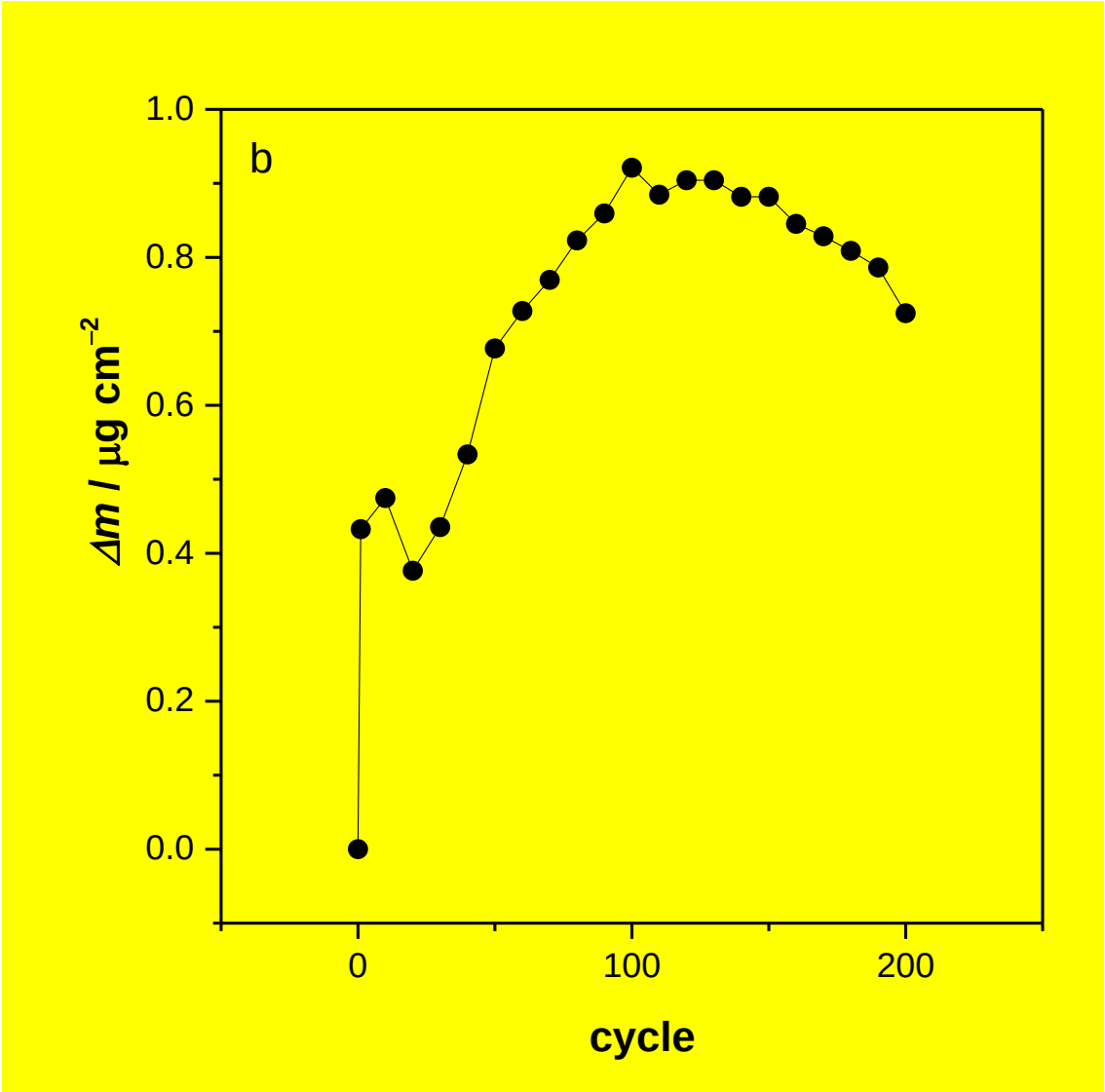


Figure 3b

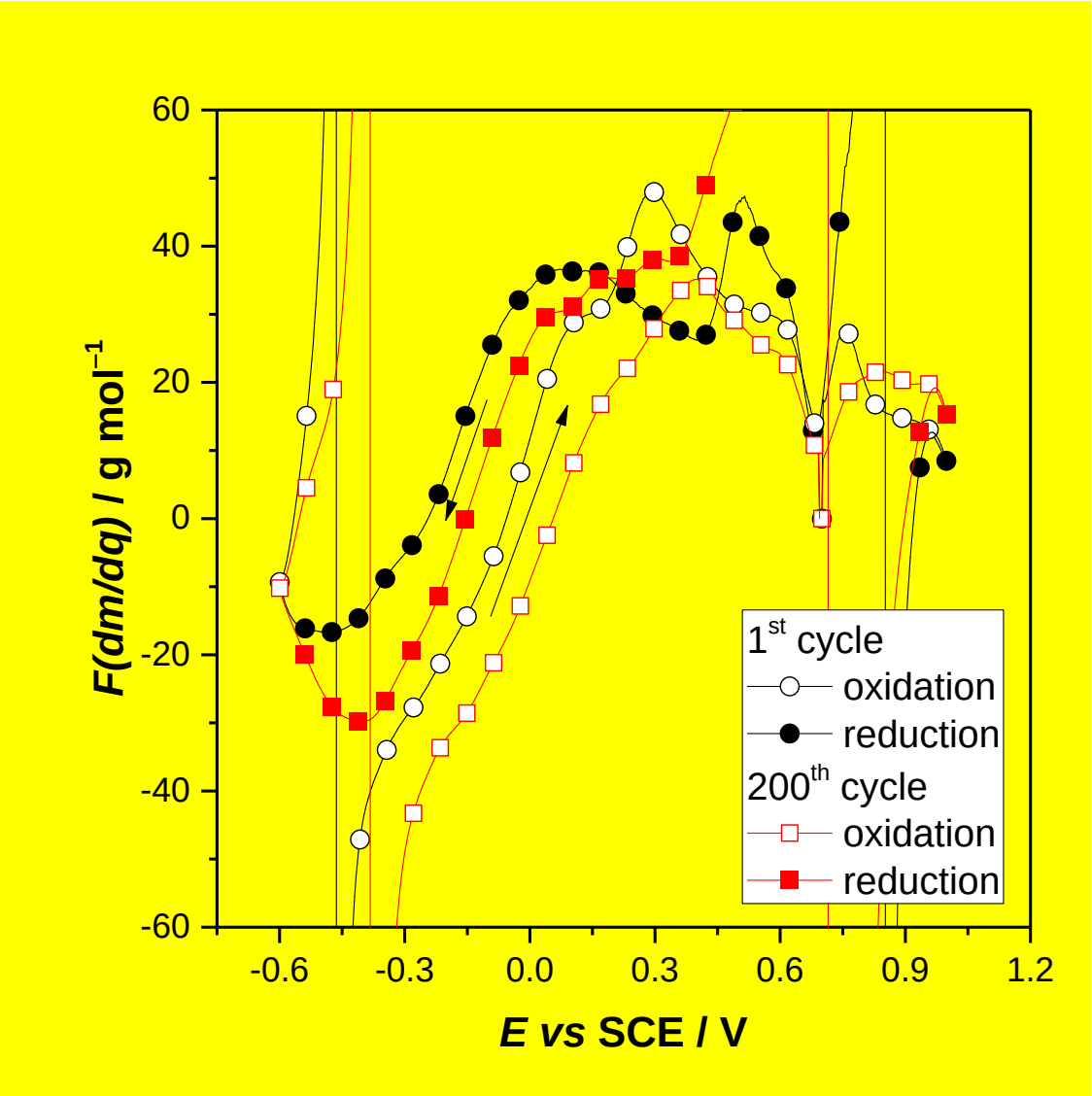
60
40
20
0
-20
-40
-60
-0.6
-0.3
0.0
0.3
0.6
0.9
1.2
F(dm/dq) / g mol⁻¹
E vs SCE / V
1st cycle
oxidation
reduction
200th cycle
oxidation
reduction

Figure 4

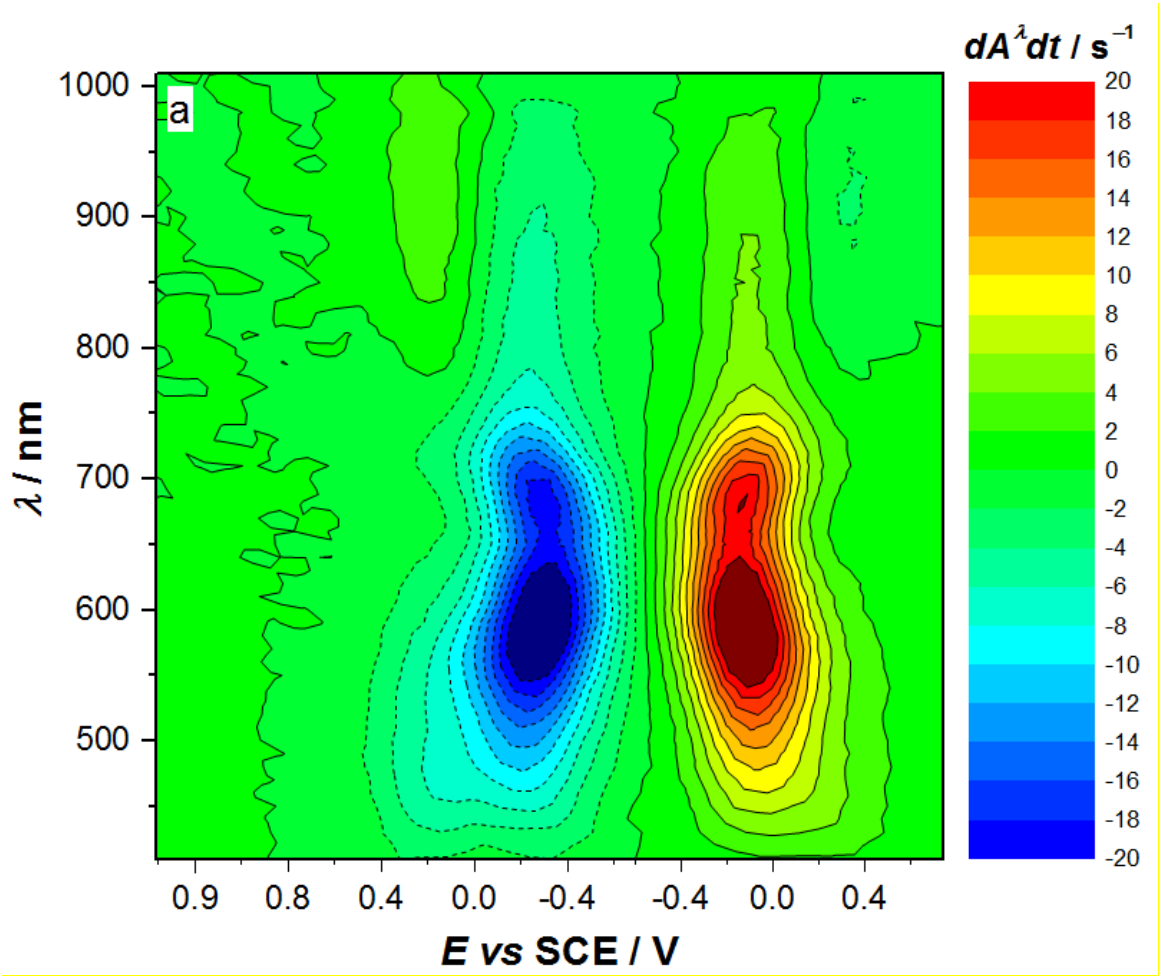
a
1000
900
800
700
600
500
λ / nm
0.9
0.8
0.4
0.0
-0.4
-0.4
0.0
0.4
E vs SCE / V
dA^λdt / s^-1
20
18
16
14
12
10
8
6
4
2
0
-2
-4
-6
-8
-10
-12
-14
-16
-18
-20

Figure 5a

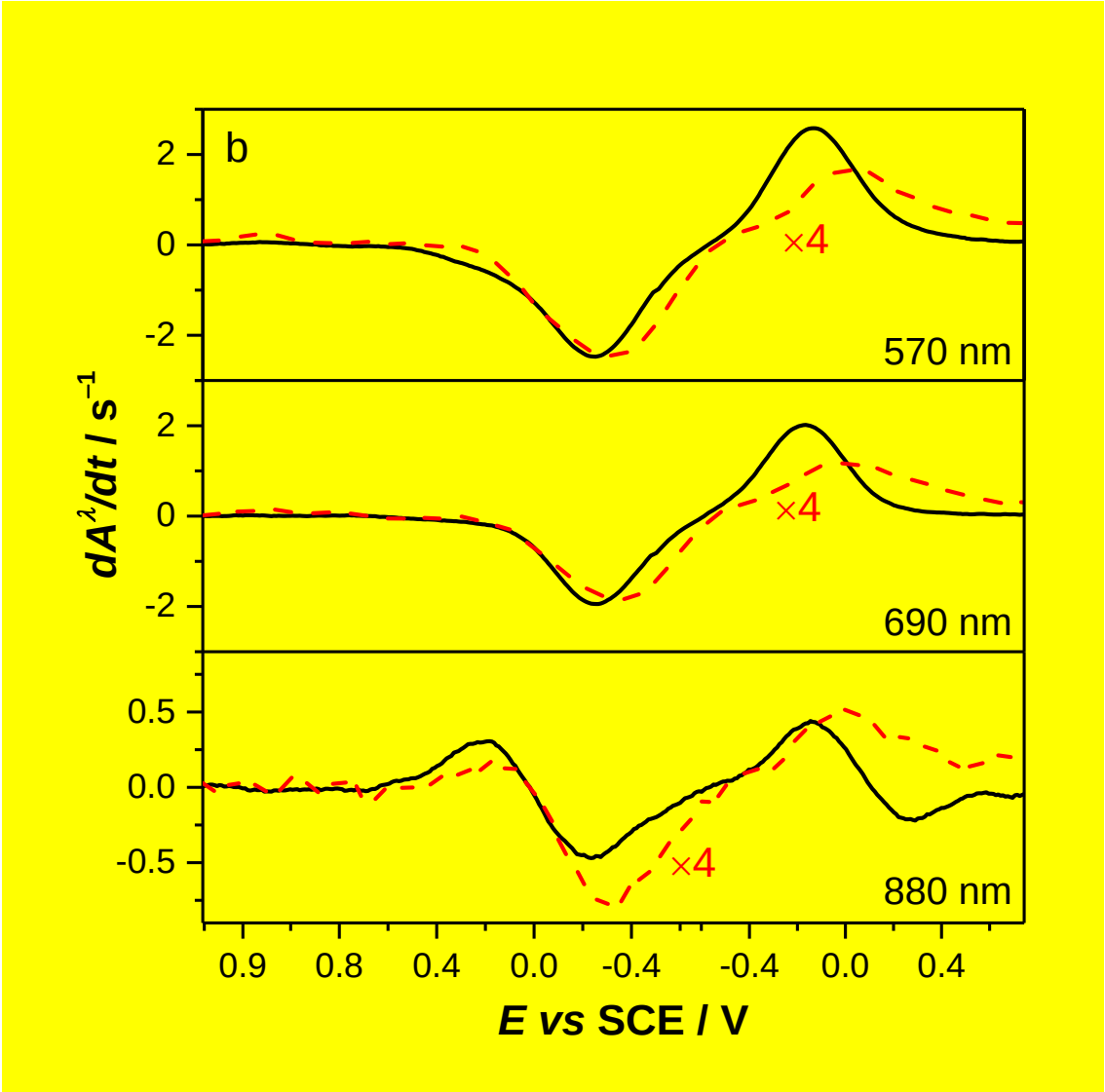
b
2
0
-2
570 nm
×4
2
0
-2
690 nm
×4
0.5
0.0
-0.5
880 nm
×4
0.9
0.8
0.4
0.0
-0.4
-0.4
0.0
0.4
E vs SCE / V
dA^½/dt / s^-1

Figure 5b

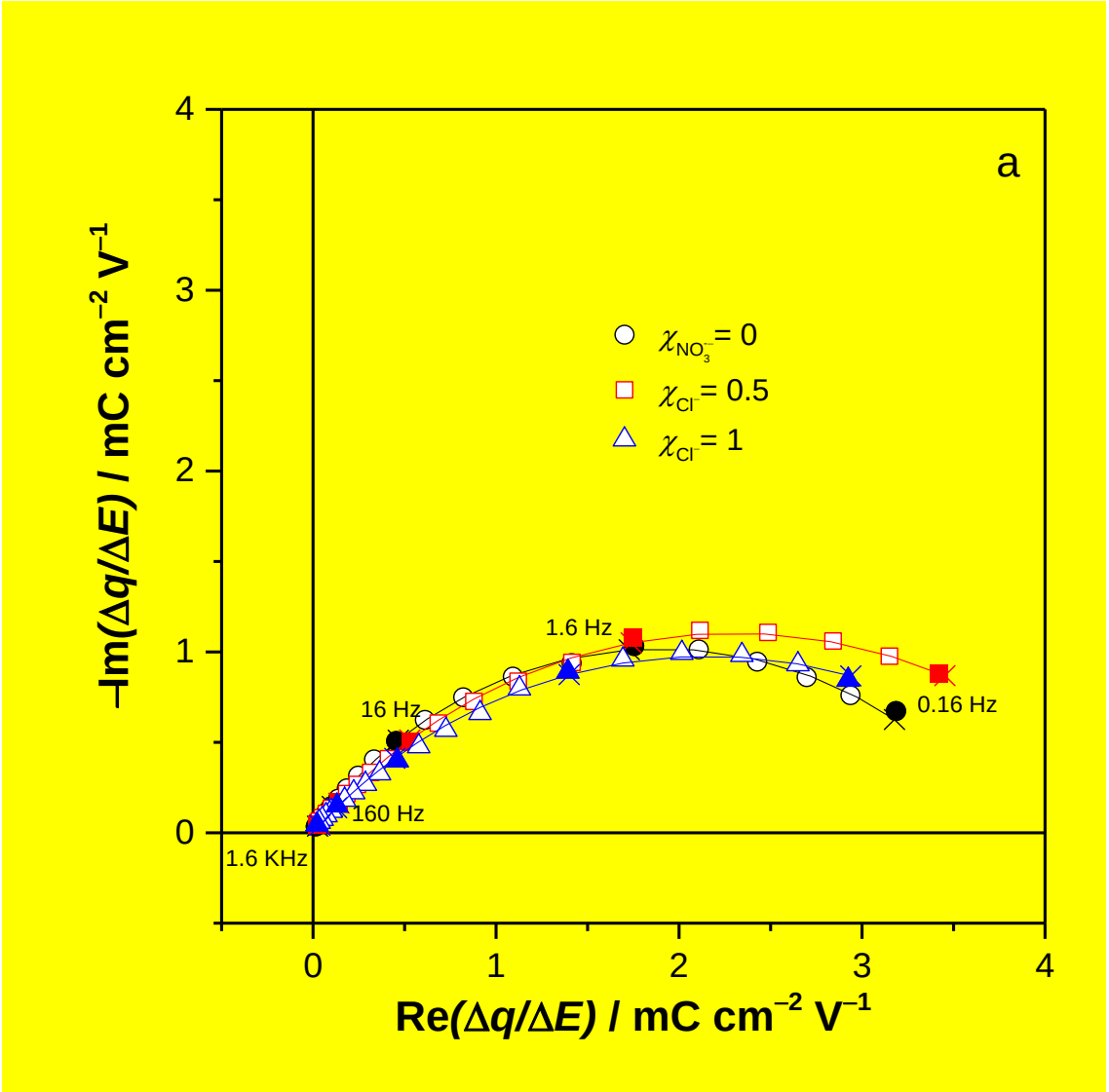
a
$\chi_{NO_3^-}$ = 0
$\chi_{Cl^-}$ = 0.5
$\chi_{Cl^-}$ = 1
1.6 Hz
16 Hz
160 Hz
1.6 KHz
0.16 Hz
−Im(Δq/ΔE) / mC cm⁻² V⁻¹
Re(Δq/ΔE) / mC cm⁻² V⁻¹
0
1
2
3
4

Figure 6a

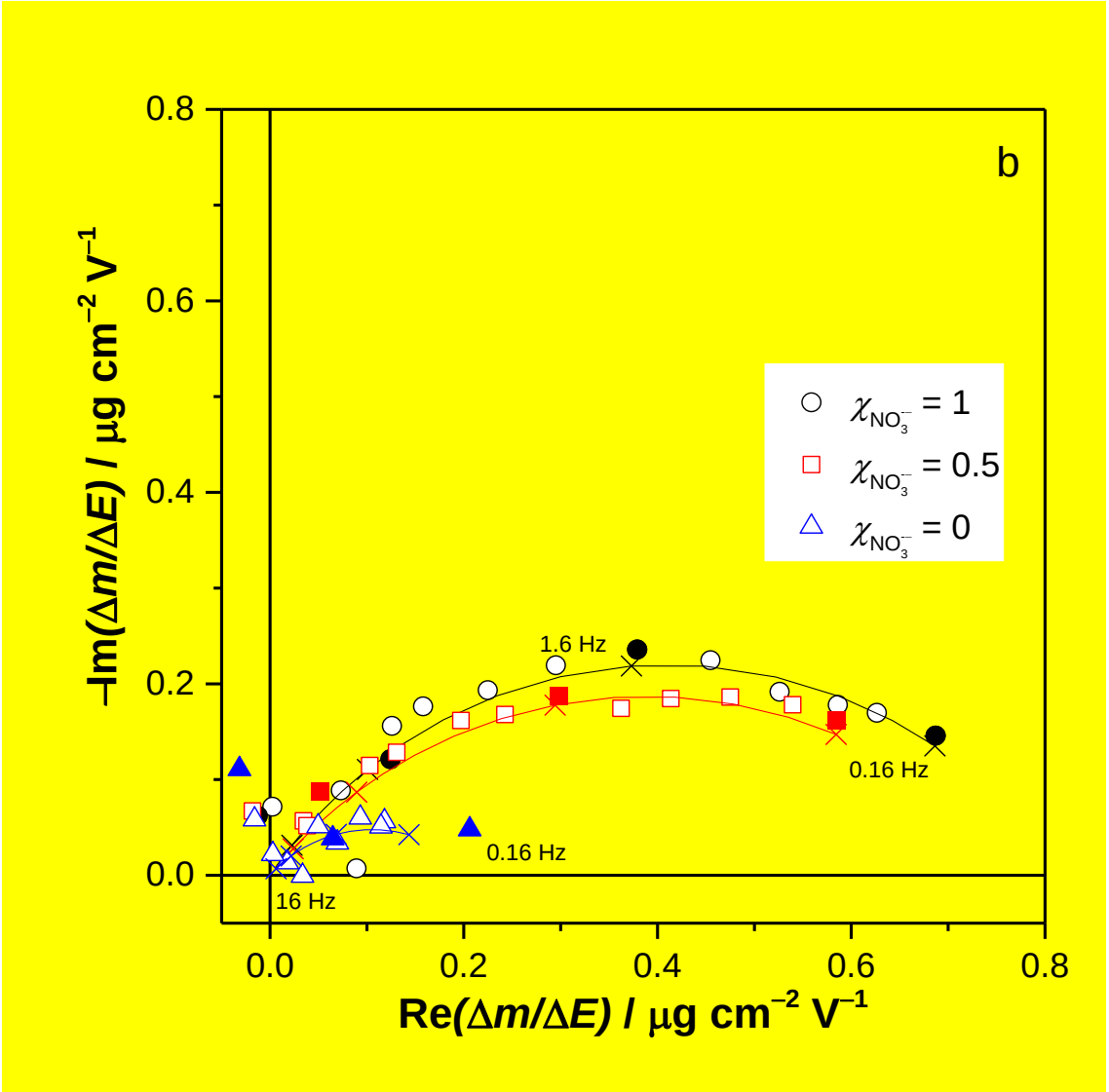
b
0.8
0.6
0.4
0.2
0.0
0.0
0.2
0.4
0.6
0.8
−Im(Δm/ΔE) / μg cm−2 V−1
Re(Δm/ΔE) / μg cm−2 V−1
χNO3− = 1
χNO3− = 0.5
χNO3− = 0
1.6 Hz
0.16 Hz
0.16 Hz
16 Hz

Figure 6b

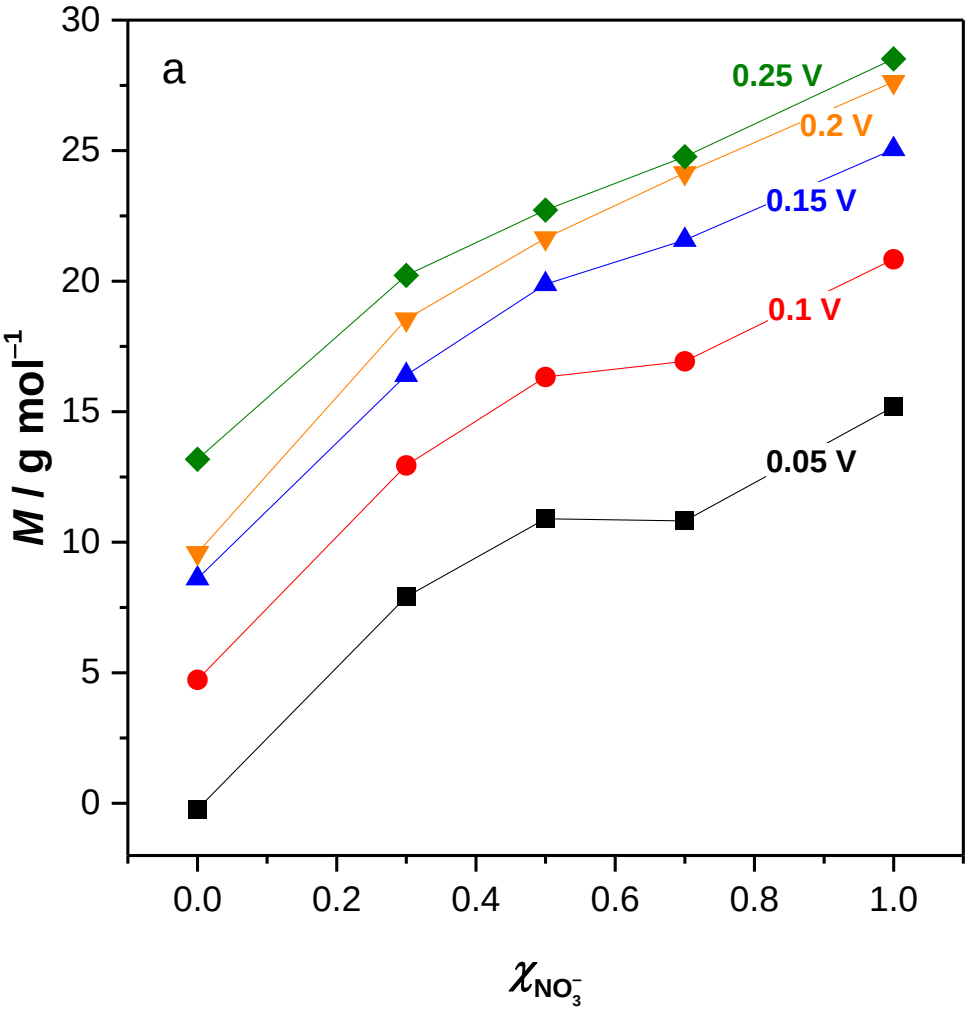
a
0.25 V
0.2 V
0.15 V
0.1 V
0.05 V
M / g mol⁻¹
χNO3⁻
0
5
10
15
20
25
30
0.0
0.2
0.4
0.6
0.8
1.0

Figure 7

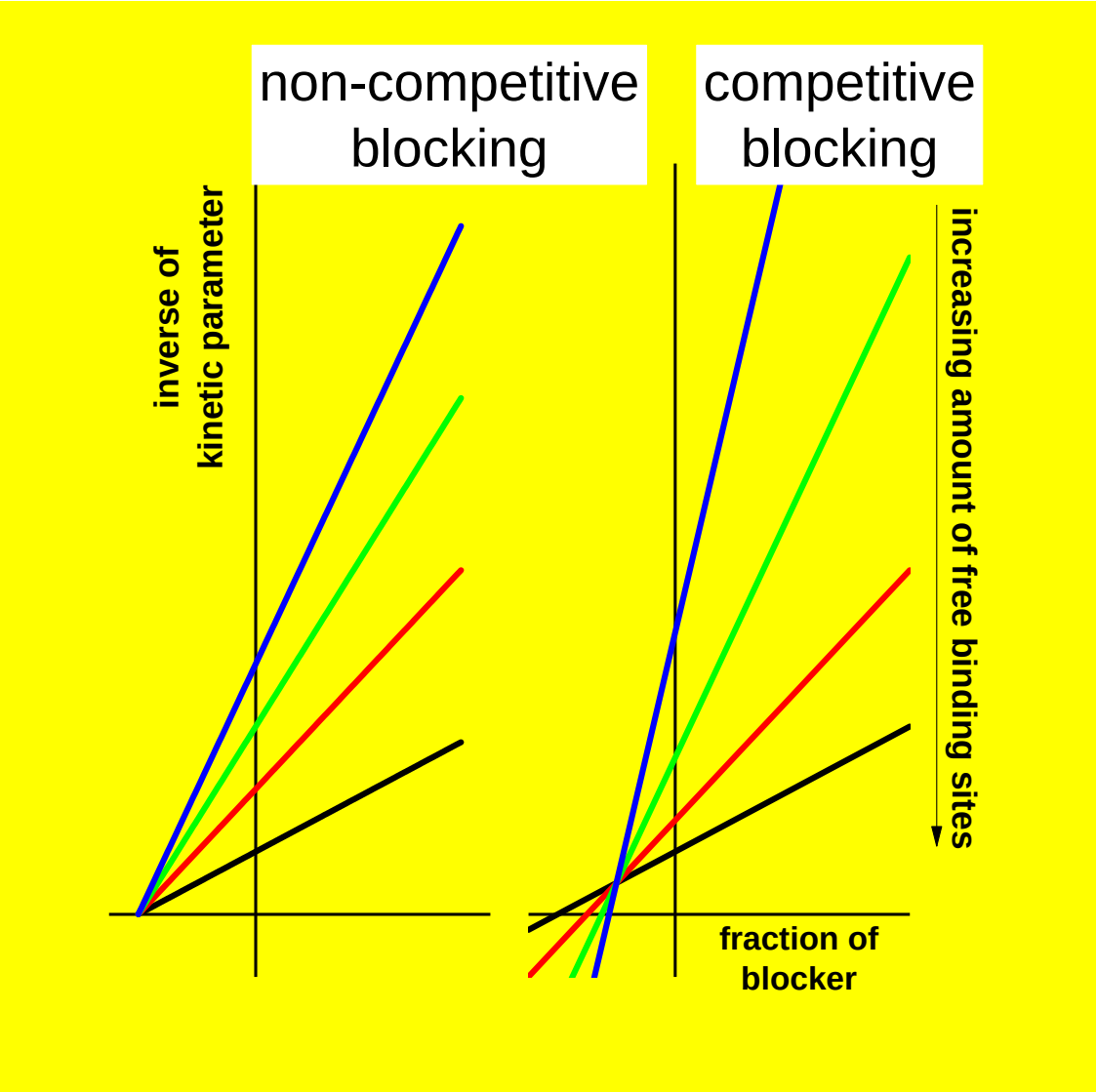
non-competitive blocking
competitive blocking
inverse of kinetic parameter
increasing amount of free binding sites
fraction of blocker

Figure 8

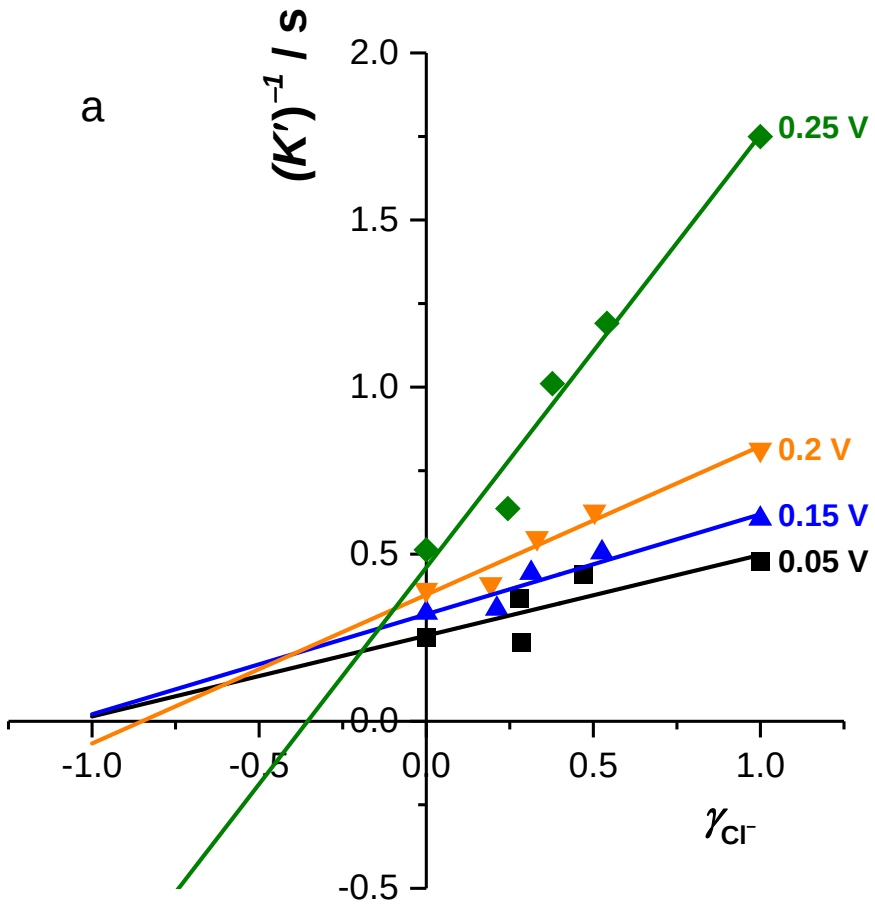


Figure 9a

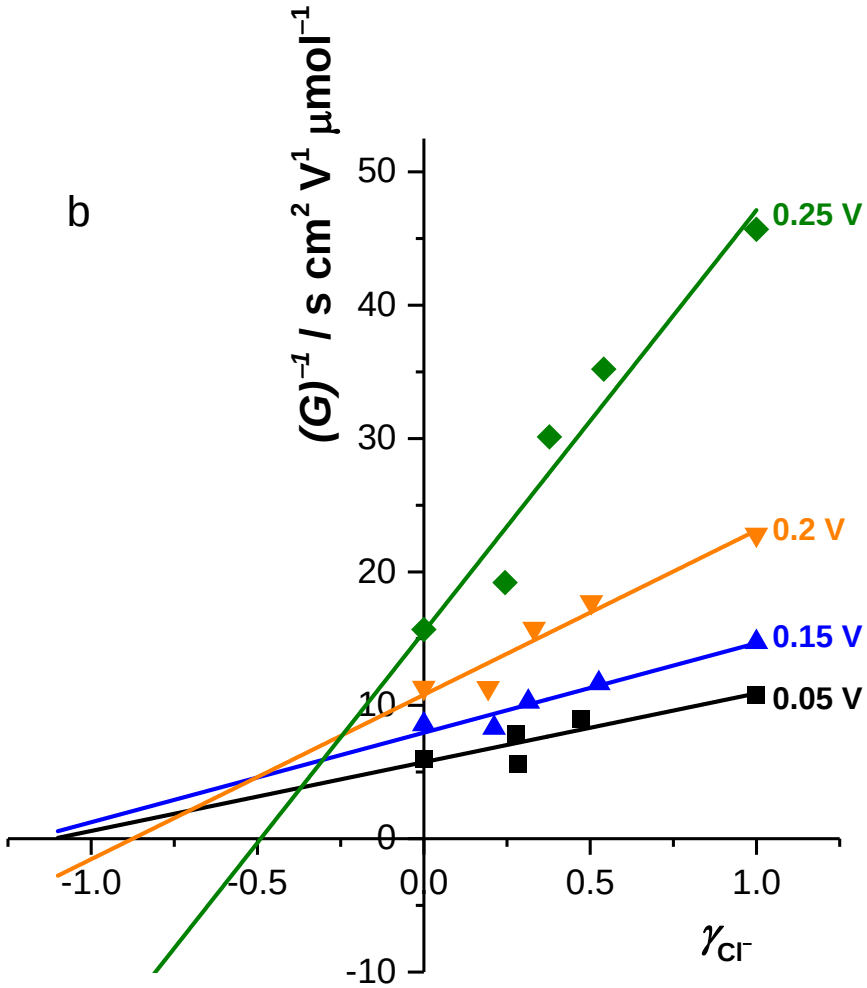
b
$(G)^{-1}$ / s cm$^2$ V$^1$ µmol$^{-1}$
50
40
30
20
10
0
-10
-1.0
-0.5
0.0
0.5
1.0
$\gamma_{Cl^-}$
0.25 V
0.2 V
0.15 V
0.05 V

Figure 9b

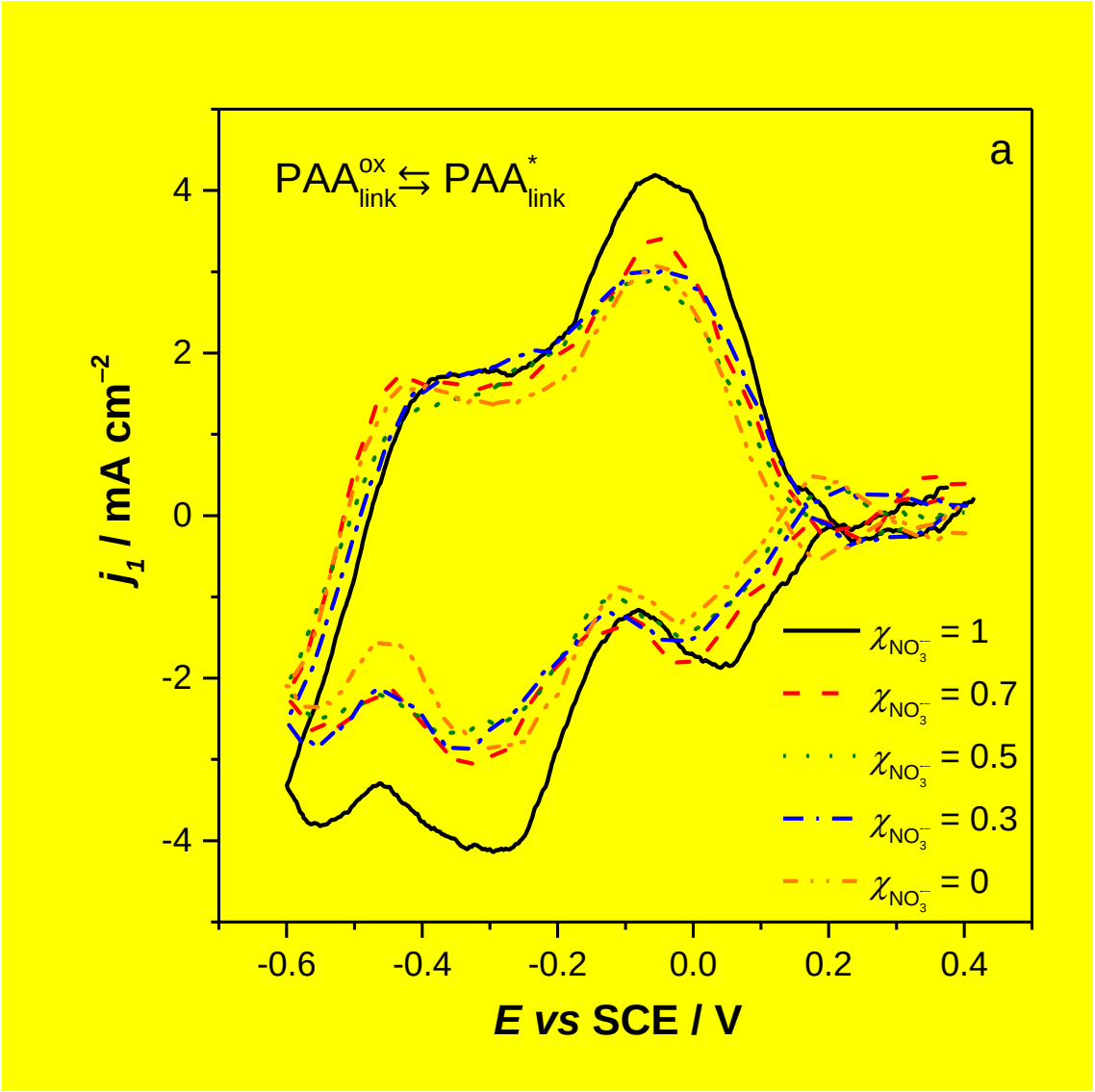
a
PAA$^{ox}_{link}$ ⇆ PAA$^{*}_{link}$
$j_1$ / mA cm$^{-2}$
4
2
0
-2
-4
-0.6
-0.4
-0.2
0.0
0.2
0.4
E vs SCE / V
$\chi_{NO_3^-}$ = 1
$\chi_{NO_3^-}$ = 0.7
$\chi_{NO_3^-}$ = 0.5
$\chi_{NO_3^-}$ = 0.3
$\chi_{NO_3^-}$ = 0

Figure 10a

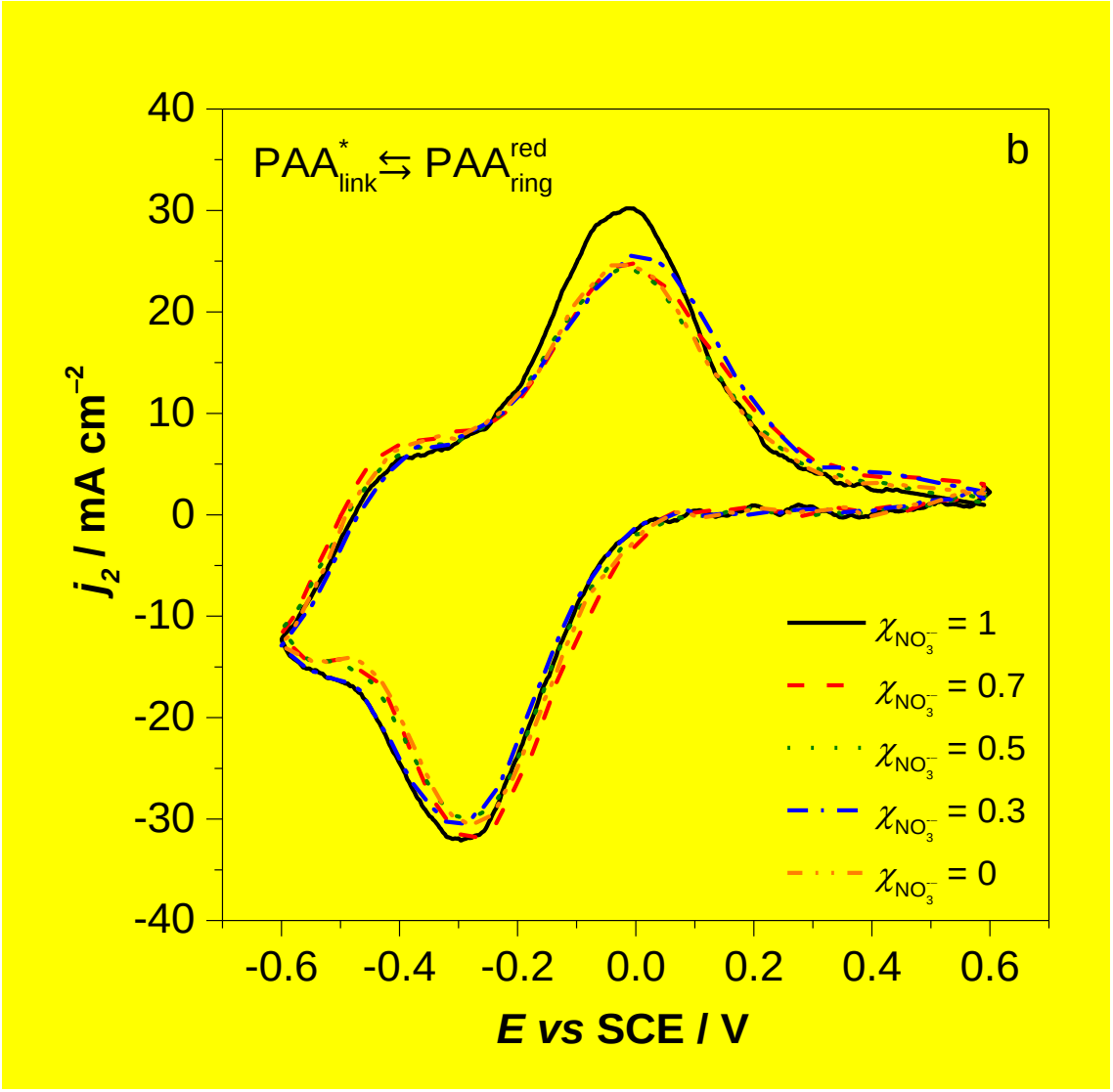
PAA*link ⇆ PAAredring
b
40
30
20
10
0
-10
-20
-30
-40
-0.6
-0.4
-0.2
0.0
0.2
0.4
0.6
j2 / mA cm−2
E vs SCE / V
χNO3− = 1
χNO3− = 0.7
χNO3− = 0.5
χNO3− = 0.3
χNO3− = 0

Figure 10b

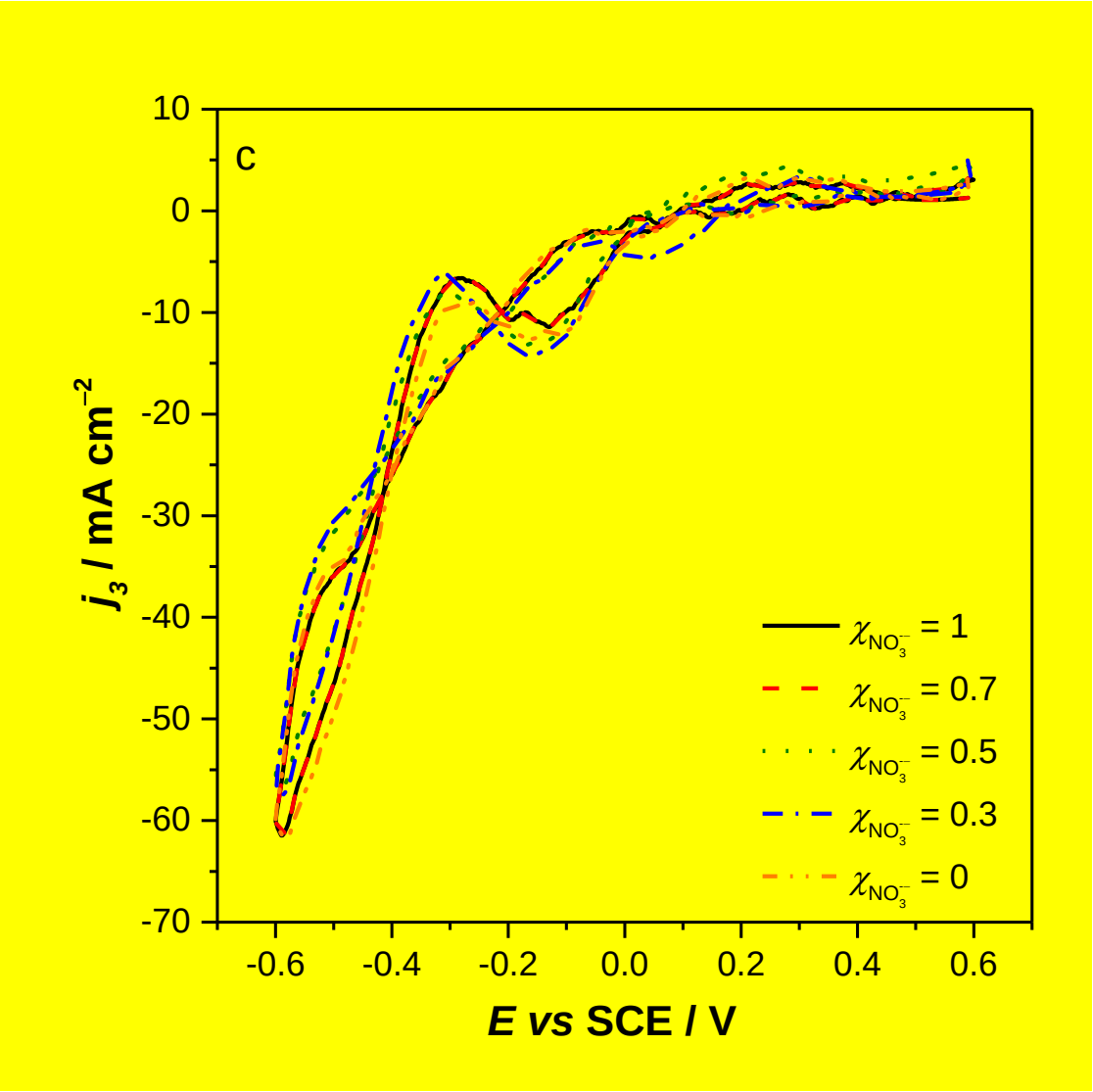
c
10
0
-10
-20
-30
-40
-50
-60
-70
-0.6
-0.4
-0.2
0.0
0.2
0.4
0.6
$j_3$ / mA cm$^{-2}$
*E vs* SCE / V
$\chi_{NO_3^-}$ = 1
$\chi_{NO_3^-}$ = 0.7
$\chi_{NO_3^-}$ = 0.5
$\chi_{NO_3^-}$ = 0.3
$\chi_{NO_3^-}$ = 0

Figure 10c